universität wien

DIPLOMARBEIT

Titel der Diplomarbeit

„NAD^+ analogues as colorigenic and fluorogenic chemical probes for NAD^+ consuming enzymes"

verfasst von

Jakob Lausch

angestrebter akademischer Grad

Magister der Pharmazie (Mag. pharm.)

Wien, 2014

Studienkennzahl lt. Studienblatt:	A 449
Studienrichtung lt. Studienblatt:	Diplomstudium Pharmazie
Betreut von:	ao. Univ.-Prof. Mag. Dr. Helmut Spreitzer

A) Acknowledgements

I am only able to submit this thesis because of many people's support.

To begin with, I would like to thank my supervisor Dr. Gerd Wagner from the Department of Chemistry and the Institute of Pharmaceutical Sciences at King's College London for the opportunity to work in his welcoming group. I am grateful for his guidance, advice and feedback on my scientific work, both in numerous group meetings and on my thesis. I am thankful for having had the chance to attend various courses, talks and symposia to expand my knowledge.

I would like to extend my thanks to Dr. Helmut Spreitzer, who has kindly agreed to act as my supervisor at the University of Vienna.

I would also like to express gratitude to all members of the Wagner group, especially Sarah Zähringer for her help with the synthesis and characterisation of nicotinamide adenine dinucleotide (NAD^+) analogues. I fully appreciate her endurance in answering my questions and thank her for introducing me to the work with NAD^+.

I extend my thanks to Jingqian Jiang, Yong Xu, Ferdinand Fuchs and Lauren Tedaldi, who all have shared their expertise and assisted me in finding solutions to many kinds of scientific problems.

I would like to thank the EPSRC National Mass Spectrometry Service Centre in Swansea for recording the mass spectra.

I gratefully acknowledge the hospitality of all people in Britannia House, who have provided a welcoming and enjoyable working atmosphere during my Erasmus stay in London.

Thanks are also due to my fellow students at the University of Vienna, who have particularly contributed to my great time at university.

Last but not least, it is a matter of particular concern to me to thank my dear friends and family for their constant support and unconditional backing throughout my entire life.

B) Abstract

NAD^+ consuming enzymes play an important role in fundamental cellular processes and have been shown to be involved in various diseases and the extension of lifespan. To understand underlying mechanisms and to find potential enzyme activators or inhibitors, the approach of chemical probes has proven to be successful on some enzymes, but broadening the applicability and discovering new probes is still an important goal.

In this project, two non-natural analogues of nicotinamide adenine dinucleotide (NAD^+), namely adenosine diphosphate ribose *para*-nitrophenol (ADPR*p*NP) and adenosine diphosphate ribose umbelliferone (ADPRumb), were synthesised, characterised and tested for their suitability as chemical probes. More precisely, after the successful acquisition of the compounds through one-pot syntheses followed by several purification steps, suitable wavelengths for absorbance assays (for ADPR*p*NP) and fluorescence assays (for ADPRumb) were determined. The compounds were tested for recognition by adenosine diphosphate ribose (ADPR) cylcase of *Aplysia californica* and NAD glycohydrolase from porcine brain. Neither of the molecules was turned over by ADPR cylcase in a continuous assay and no cleavage from ADPR*p*NP could be detected when incubated with NAD glycohydrolase in a discontinuous assay. ADPRumb showed low conversion (2 %) by NAD glycohydrolase under the tested conditions (0.012 U/mL, pH 8.0, 37 °C, 4 h), limiting its usage as a chemical probe for NAD glycohydrolase.

Neither of the tested compounds showed significant potential to serve as a chemical probe for ADPR cyclase or NAD glycohydrolase.

C) Zusammenfassung

NAD^+ konsumierende Enzyme spielen eine wichtige Rolle in fundamentalen zellulären Prozessen und es wurde gezeigt, dass sie an verschiedenen Krankheiten und der Verlängerung der Lebensspanne beteiligt sind. Um die zugrunde liegenden Mechanismen zu verstehen und potenzielle Enzymaktivatoren oder –inhibitoren zu finden, hat sich der Ansatz der chemischen Untersuchungsmoleküle (chemical probes) bei manchen Enzymen als erfolgreich herausgestellt. Ein wichtiges Ziel besteht noch immer darin, deren Anwendbarkeit zu erweitern und neue Untersuchungsmoleküle zu entdecken.

In diesem Projekt wurden zwei künstliche Analoga von Nikotinamid-Adenin-Dinukleotid (NAD^+), nämlich Adenosindiphosphat-Ribosyl-*para*-Nitrophenol (ADPR*p*NP) und Adenosindiphosphat-Ribosyl-Umbelliferon (ADPRumb), synthetisiert, charakterisiert und auf ihre Eignung als chemische Untersuchungsmoleküle getestet.

Nach erfolgreicher Herstellung der Verbindungen über jeweils Ein-Topf-Synthesen und mehrere Reinigungsschritte wurden geeignete Wellenlängen für Absorptionstests (bei ADPR*p*NP) und Fluoreszenztests (bei ADPRumb) bestimmt. Die Verbindungen wurden auf Erkennung von Adenosindiphosphat-Ribosyl (ADPR) Zyklase von *Aplysia californica* und NAD Glykohydrolase aus Schweinehirn untersucht. Keines der Moleküle wurde von ADPR Zyklase in einem kontinuierlichen Testsystem umgesetzt und es konnte keine Spaltung von ADPR*p*NP durch NAD Glykohydrolase in einem diskoniuierlichen System bemerkt werden. ADPRumb zeigte geringe Umsetzung (2 %) durch NAD Glykohydrolase unter den Testbedingungen (0.012 U/mL, pH 8.0, 37 °C, 4 h), was die Nutzung dieser Verbindung als chemisches Untersuchungsmolekül für NAD Glykohydrolase limitiert.

Keine der getesteten Verbindungen zeigte signifikantes Potenzial, als chemisches Untersuchungsmolekül für ADPR Zyklase oder NAD Glykohydrolase zu dienen.

D) Table of Contents

E) Introduction

E.1) NAD^+ and metabolites thereof

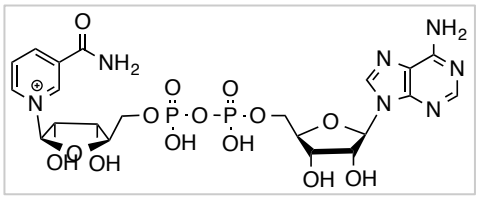

Figure 1: structural formula of NAD^+

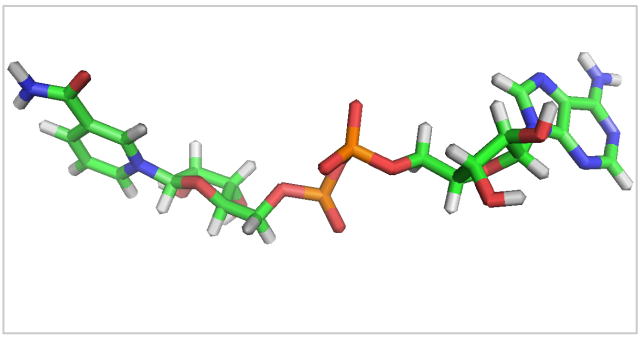

Figure 2: NAD^+ depicted in the conformation bound to SIRT1[1]

(H, grey; C, green; O, red; N, blue; P, orange)

Nicotinamide adenine dinucleotide (NAD^+, see Figure 1 and Figure 2) is a biomolecule found in all living cells[2] and has long been recognised as a coenzyme involved in many intracellular redox processes, changing between oxidised (NAD^+) and reduced (NADH) form[3]. In the 1960s, another property of this remarkable molecule, incorporating both energy and signal transfer, was discovered: researchers began to realise that NAD^+ also serves as a substrate for NAD^+ consuming enzymes, leading to the cleavage of the energy rich N-glycosidic bond releasing nicotinamide[4].

Up to now, several different enzymes causing this bond to break have been discovered and can be classified according to their main product.

Table 1: NAD^+ consuming enzymes: catalysed reactions and examples[5]

catalysed reaction	**examples**
formation of ADPR (via hydrolysis)	NAD glycohydrolase, CD38[6] (cluster of differentiation)
automodification (cyclisation)	ADPR cyclase[6]
protein modification	poly (ADPR) polymerases (PARPs)
	mono (ADPR) polymerases
	NAD^+-dependent deacylases
nucleic acid modification	NAD^+-dependent tRNA 2'-phosphotranserases
small molecule modification	bacterial CobT (involved in cobalamin biosynthesis)
	mycobacterial rifampin ADPR transferase (involved in rifampin inactivation)[7]

Many of these enzymes are essential players in fundamental cellular processes. Therefore, researchers have sought different approaches to study their enzymatic activity and, as some enzymes are known to be involved in diseases, have tried to manipulate their behaviour. Since many enzyme substrates or products are not directly quantifiable, one possible strategy to study enzymes is measuring their activity against chemically modified analogues of natural substrates, i.e. using chemical probes. An ideal chemical probe for enzymological purposes should be easily accessible, giving a quantifiable readout, and having an enzymatic recognition pattern similar to the physiological substrate, to name but a few.
The focus of this work was on ADPR cyclase of *Aplysia californica* and NAD glycohydrolase from porcine brain.

E.2) ADPR cyclase and ADPR cyclising enzymes

The ectoenzyme CD38[8] is considered to be the main ADPR cyclase in mammals and catalyses two reactions involving the substrate NAD^+ at neutral pH[9]. On incubation with NAD^+, a small portion is cyclised to cyclic adenosine diphosphate ribose (cADPR), whereas the majority is hydrolysed to ADPR. Additionally, CD38 facilitates the cleavage of cADPR to ADPR. (It is also known to convert NADP to NAADP under acidic conditions, but this work focuses on NAD^+ consuming enzymes.)

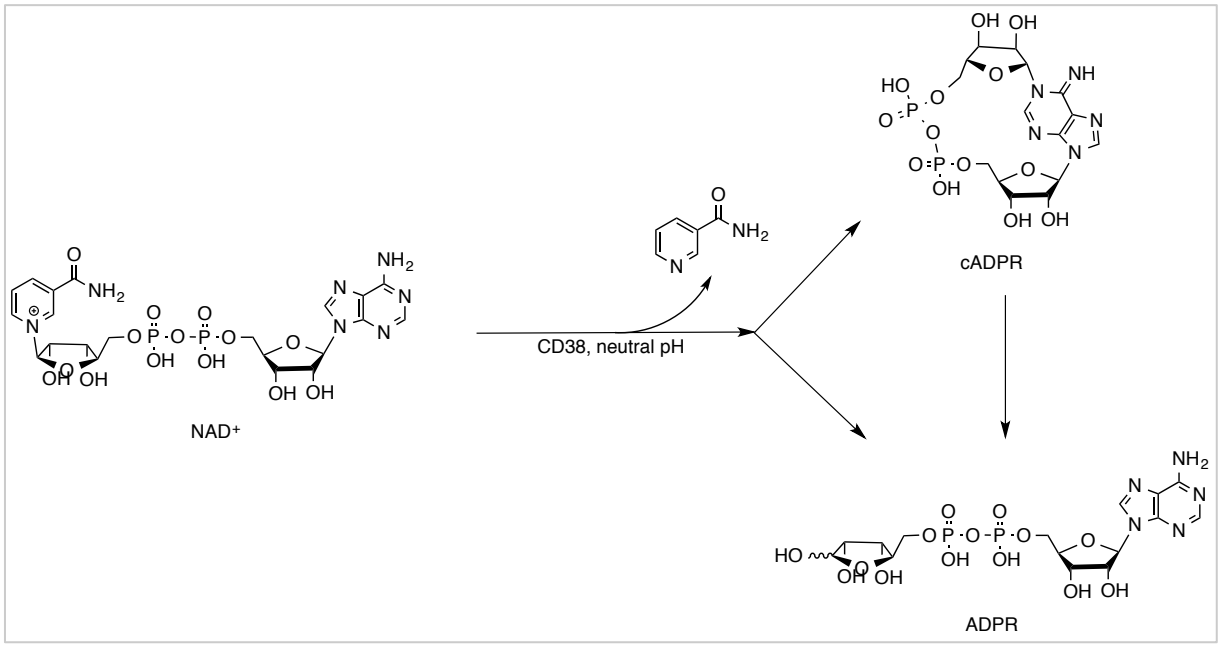

Figure 3: schematic of the reaction catalysed by CD38 at neutral pH

CD38 and cADPR are known to play an important role in Ca^{2+}-mobilisation, especially in the calcium induced calcium release (CICR) from the endoplasmic reticulum, probably via interaction with the ryanodine receptor[9]. Research has shown that CD38 is involved in morphine mediated antinociception[10], inflammatory processes (e.g. in age related macula degeneration[11]), neuronal differentiation and proliferation[12], insulin secretion[13] and cardiac function[14]. Hence, intervening in cADPR formation seems an interesting approach for treatment of various diseases in these areas.

On the second possible product, ADPR, less work has been published. Involvement in Ca^{2+}-trafficking has been observed, both via the transient potential receptor melastatin-2 (TRPM2)[15] and the purinergic receptor P2Y1[16], but the detailed mechanisms of signal transduction still remain to be clarified.

The fundamental role of the products of ADPR cyclase gives reason for investigating the mechanisms of this enzyme and for modifying its activity.

In order to develop drugs targeting ADPR cyclase, an appropriate assay is essential. ADPR cyclase of *Aplysia californica*[17] is a commercially available homologue of CD38, having similar structural features[9]. It is, therefore, worthwhile developing enzyme assays using this homologue.

E.3) NAD glycohydrolase

NAD glycohydrolase from porcine brain has long been known for its ability to catalyse the hydrolysis of the N-glycosidic bond between the nicotinamide and the ribose in NAD^+ to form ADPR[18].

It is a commercially available member of the class of NAD glycohydrolases, which are also called NADases, an inaccurate name because all NAD^+ consuming enzymes cleave NAD^+ per definition. Additionally, there is a growing body of evidence that the group is heterogeneous in terms of catalytic behaviour and members of the NAD glycohydrolases have been shown to cyclise NAD^+ to form cADPR, although in a very low yield[19]. Some members of the former coherent group have been suggested to have additional catalytic properties, similar to the cyclising activity of CD38[20].

Up to the present day, it is not clear whether NAD glycohydrolase from porcine brain purely forms ADPR or also cADPR. In either case, reaction products of this enzyme are involved in fundamental cellular processes, making the enzyme an interesting target for further studies.

E.4) Sirtuins

The most recently discovered NAD^+ consuming enzymes are named sirtuins, an enzyme class whose members are found in all phyla of life, including viruses[21]. They all share the common feature of catalysing deacylation reactions of proteins, and some have been reported to act as mono-ADP-ribosyltransferases, too. Figure 4 shows the reaction scheme of one example of sirtuin-catalysed reactions, the deacetylation of a lysine residue.

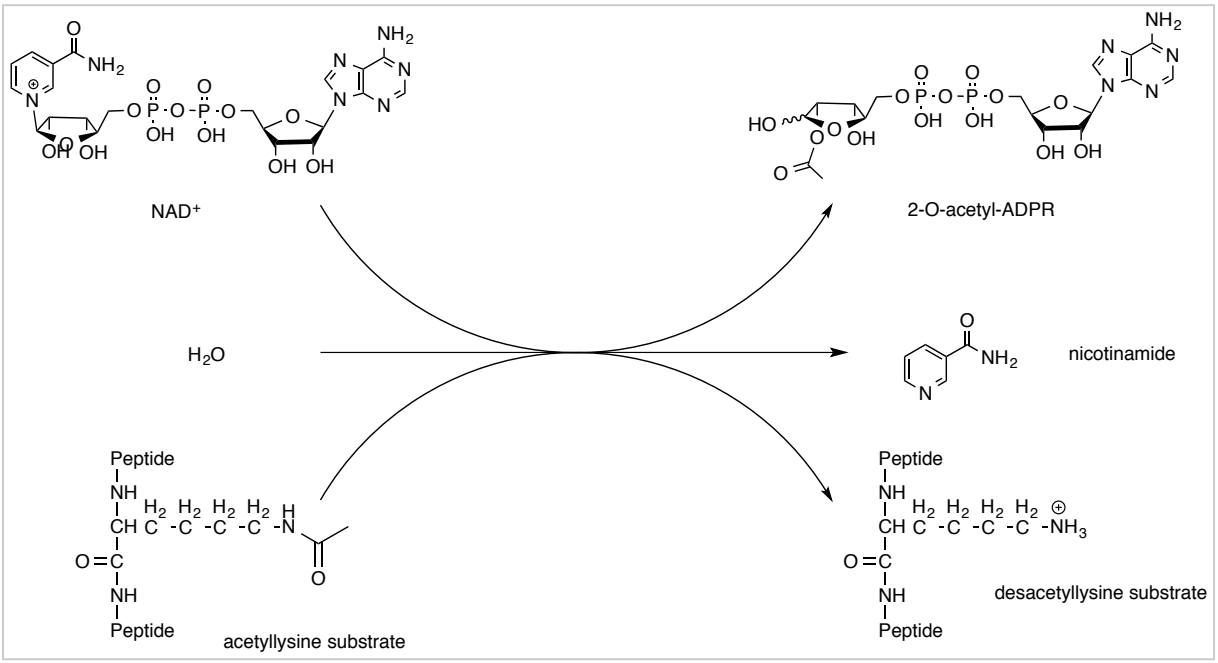

Figure 4: reaction scheme of NAD$^+$-dependent deacetylation of a lysine residue, an example of a general deacylation catalysed by sirtuins[21]

The best-studied mammalian sirtuin is SIRT1, out of 7 in total, acting as a deacetylase on various substrates, which can result in either transcriptional activation or inhibition[22]. Its involvement in mitochondrial biogenesis through peroxisome proliferator activated receptor γ coactivator (PGC)-1a; metabolism of lipids and carbohydrates via peroxisome proliferator activated receptors (PPARs), sterol regulatory element binding protein (SREBP)-1, liver X receptor (LRX), cAMP response element binding protein (CREB); and cell proliferation via p53 demonstrates the fundamental role of SIRT1 in cell physiology[23]. Moreover, SIRT1 activity has been linked to increased life- and healthspan, depending on the spatial distribution and the extent of its overexpression[24].

To study these mechanisms more in-depth and to pharmacologically manipulate pathways of SIRT1, selective and sensitive sirtuin assays are in great demand. Existing assays tend to show shortcomings, which indicate the need for alternatives.

The initial assays made use of radioactively labelled histones or chemically [^{3}H]-acetylated oligopeptides[25], having the disadvantage of expensive preparation of substrates, the need of special safety measures for laboratory personal and careful waste disposal.

The use of oligopeptides incorporating a C-terminal acetyl-lysine-coumarinylamide that could be cleaved by trypsin only upon deacetylation and could then be detected by fluorescence overcame the drawbacks of radioactive assays. Nevertheless, after several

years in use, it was shown that the application of coumarine-labelled substrates could act as artificial substrates and therefore render impossible the drawing of sensible conclusions[26].

Recently, a new method has been published using the enzymatic conversion of nicotinamide, the by-product of NAD^+ consuming enzymes, to ammonia, which, in turn, can be detected spectrophotometrically after another enzymatic conversion[27]. For high throughput screening of potential inhibitors, an assay using more than one enzyme is less selective; therefore, a testing system necessitating only the enzyme of interest is favourable.

F) Previous corresponding work and aim of the project

The instability of the N-glycosidic bond between nicotinamide and the ribose under alkaline aqueous conditions has long been known[28], and the hydrolysis of this bond has been studied extensively[29]. Nevertheless, very little is known about the reaction behaviour in dimethyl sulfoxide (DMSO).

Previously, metal halides in DMSO and triethylamine (TEA) have been successfully used to selectively remove the nicotinamide moiety of NAD^+ from the anomeric carbon and to achieve a nucleophilic attack on the same carbon atom.[30] In light of this technique, the synthesis of ADPR*p*NP has been conducted before[31]. In a straightforward one-pot synthesis, *para*-nitrophenol (*p*NP) was attached to the ADPR scaffold in its deprotonated and thus more nucleophilic form. Interestingly, the new bond was found to be only in β-configuration, according to the measurement of the Nuclear Overhauser effect (NOE) between H-1'' and H-2'' on the ribose where the new bond had just been formed[31].

ADPR*p*NP has been shown to be a colorigenic substrate for some PARPs, a family of NAD^+ consuming enzymes[31], raising the question whether this molecule could serve as a chemical probe for a broader range of NAD^+ consuming enzymes using the measurement of specific absorbance changes during the incubation.

Fluorescence measurement is known to be more sensitive than absorbance quantification, and, given the fact that each fluorophore has characteristic excitation and emission properties, it is more selective, too. A fluorogenic chemical probe would, consequently, transfer these advantages to enzymology.

The fluorescence properties of coumarines are commonly known and those of the phenolic umbelliferone have been studied with regard to pH in great detail[32]. Using the simplest phenolic derivative, one can expect fluorescence and synthetic behaviour similar to *p*NP.

In this work, the previously reported one-pot synthetic strategy was applied to produce the potentially colorigenic substrate ADPR*p*NP and it was adapted to form the potentially fluorogenic substrate ADPRumb.

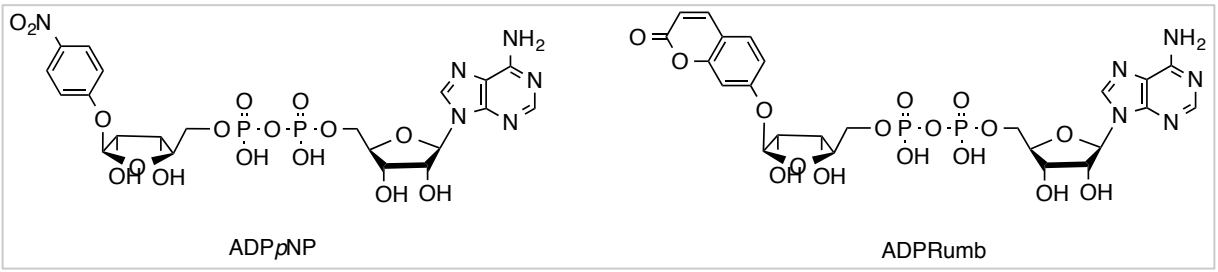

Figure 5: structures of target molecules

These two molecules were purified, characterised and tested on their ability to serve as substrates for NAD glycohydrolase from porcine brain and ADPR cyclase from *Aplysia californica*.

This avenue has several advantages, both synthetic ones and ones in terms of assay development. A one-pot synthesis avoids various reaction and purification steps, making the synthesis much easier and efficient with respect to time and money.

With regard to the assay development, in situ generation of specific absorbance or fluorescence properties is easily detectable by a plate reader, facilitating the direct and immediate measurement of a biochemical reaction. Hence, the enzyme kinetics can be studied smoothly due to continuous formation of chromophore or fluorophore, and, if necessary, in a high throughput assay. One inherent limitation of this testing setup is the fact that the assay cannot be applied to other NAD^+ consuming enzymes without prior confirming the enzyme's recognition of the alternative substrate. Nevertheless, the usage of only one enzyme in a screening of potential inhibitors or activators ascertains the selectivity of the assay besides the advantage of a continuous readout.

G) Results and discussion

G.1) Synthesis of ADPR*p*NP

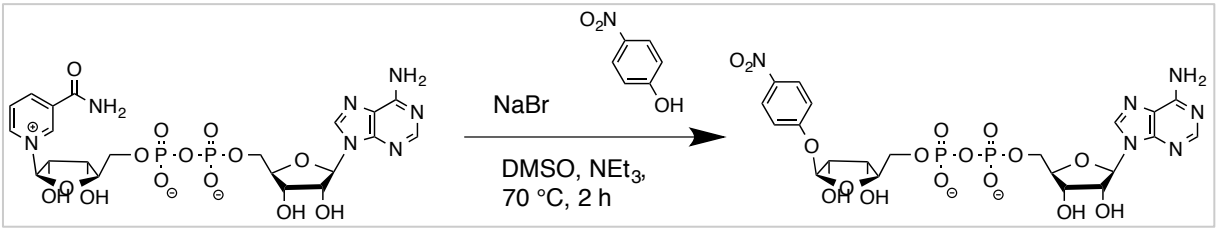

Figure 6: reaction scheme of the synthesis of ADPR*p*NP

The aim of this reaction was the exchange of the positively charged and thus good leaving group nicotinamide for the nucleophile *p*NP.

Since NAD^+ is a very labile compound in aqueous solution under basic conditions, the reaction was performed in anhydrous DMSO under a protecting atmosphere of N_2 to avoid hydrolysis. NaBr was used as an activating agent, interchanging the quaternary pyridinium ion with a bromide. NaBr has proven the most suitable of several alkali halides for cleaving the N-glycosidic bond[30]. It is still unknown what the nature of the glycosyl halide bond in the intermediate structure is in DMSO. An oxocarbenium intermediate has been proposed in aqueous hydrolysis simulation[29], but a nucleophilic substitution in DMSO has never been examined. Nevertheless, taking advantage of the one pot strategy in order to provide a sufficing amount of product, it was not vital to examine the intermediate. TEA, serving as a base, deprotonated *p*NP (colour change to bright yellow) to render it more nucleophilic, and as such being able to attack the anomeric carbon of the terminal ribose to form an O-glycoside.

The reaction temperature of 70 °C and the reaction time of 2 h were chosen as a compromise between obtaining enough product and avoiding degradation products. Especially the pyrophosphate bond is known to be labile under basic conditions after cleavage of the N-glycoside between the ribose and the nicotinamide[33].

Since the purpose of this work was to synthesise a sufficient amount of material to characterise the compound and conduct enzymatic assays, working out the optimum reaction conditions and investigating various side products was considered negligibly.

After the successful detection of product on thin layer chromatography (TLC), excess DMSO was removed by rotary evaporation before purification by reversed phase (RP) - chromatography and subsequent ion exchange chromatography yielding a slightly yellow powder.

Due to the direct approach of this reaction, complex protecting and deprotecting of various functional groups was avoided, giving this method a distinct advantage over conventional synthetic routes, which might involve the new formation of the pyrophosphate bond.

Various methods were used to confirm the structure of the compound, including nuclear magnetic resonance (NMR) spectroscopy. Generally, the observed data fitted the expected features of the molecule, but due to overlapping signals of the riboses, not every coupling could be detected in the ^{1}H-NMR. It is commonly known that quaternary carbons can give very small signal intensities in ^{13}C-NMR experiments, which can, depending on the resolution, lead to them not being observed in the spectra. That fact could explain why only 20 out of 21 expected carbons were seen in the spectrum. The ^{31}P-NMR confirmed the intact pyrophosphate bond (multiplet at δ -11.11 – -11.63 ppm, comprising 2 P), because a cleavage would have given a terminal phosphate and, consequently, a shift further downfield[34]. The separation process and TLC in combination with the NMR measurements ensured that the O-glycosidic bond between *p*NP and the terminal ribose of ADPR had been formed.

The configuration of the newly formed bond was assigned by determining the relative distance between H-1'' and H-4''. In β-configuration these two protons are on the same side of the furanose-ring, ergo closer to one another than in α-configuration where they are on opposing sides (see Figure 7). Furthermore, in β-configuration, H-1'' is closer to H-4'' than to H-3'', as opposed to α-configuration.

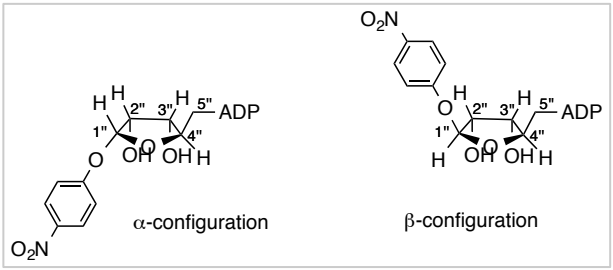

Figure 7: structural formula of ADPR*p*NP in α- and β-configuration

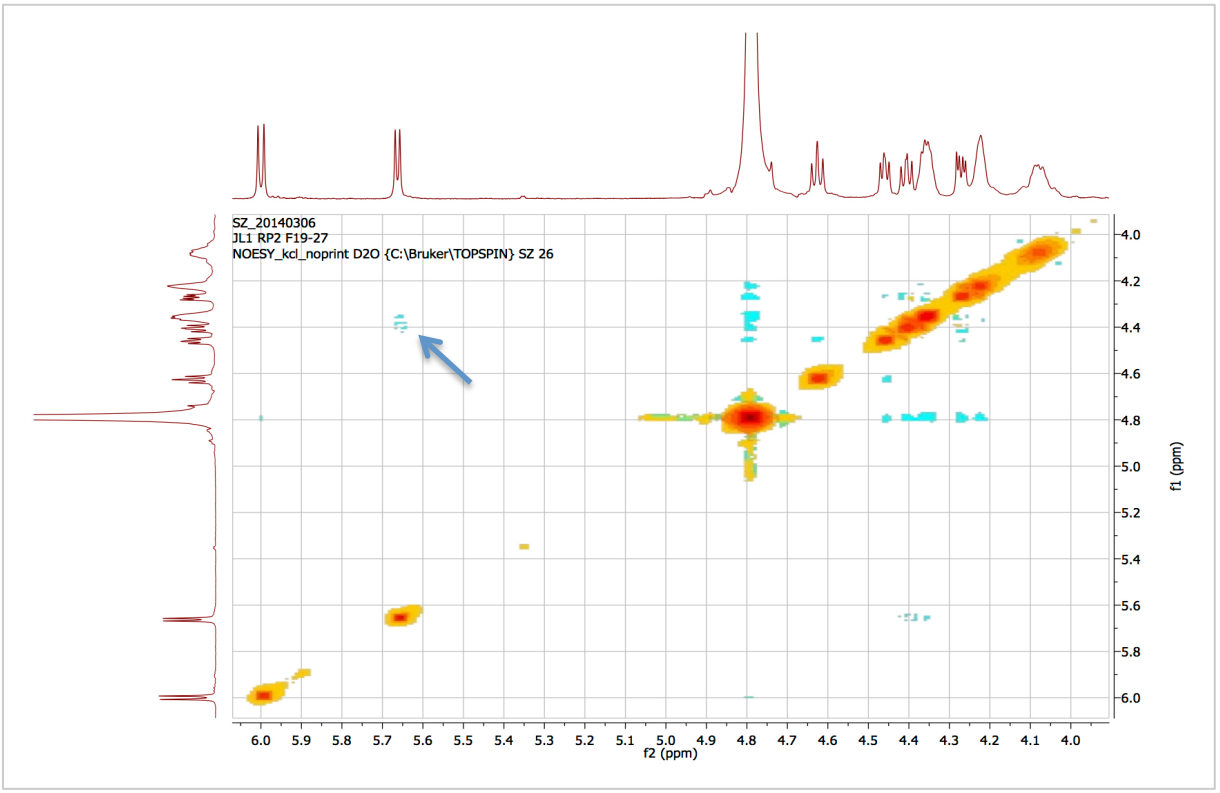

Figure 8: NOESY of ADPR*p*NP.

The arrow indicates the cross peaks of H-1'' with H-2'' and H-4'' but not H-3'', confirming β-configuration. The yellow to red colour depicts the positive crosspeaks (mostly diagonal peaks); the turquoise peaks show negative crosspeaks (peaks due to NOE).

The Nuclear Overhauser effect spectroscopy (NOESY) experiment (Figure 8) shows the assignment of the configuration due to the fact that H-1'' (5.66 ppm) couples more strongly with H-2'' (4.41 ppm) than with H-4'' (4.39 – 4.32 ppm), but still visible, and not with H-3'' (4.27 ppm).

Another NOESY experiment was performed on commercially available β-NAD^+, showing similar coupling signals, indicating that β-conformation can be assigned according to the NOESY peaks. Although the resolution was not ideal, the reaction conditions used in this synthesis have yielded β-configured products in other experiments before [30,31].

The mass spectrum was another proof for the successful synthesis, showing the main peak at m/z = 339.0358, which corresponds to the twice deprotonated form with a theoretical m/z = 339.0367

G.2) Synthesis of ADPRumb

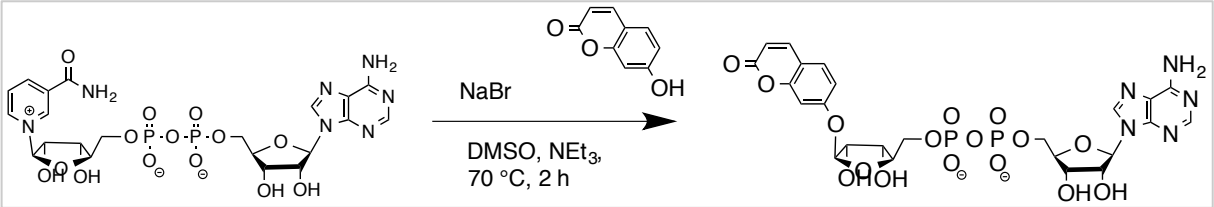

Figure 9: reaction scheme of the synthesis of ADPRumb

Adapting the protocol for the formation of ADPR*p*NP, the same conditions were used to synthesise ADPRumb.

After the addition of TEA, the reagent mixture turned yellow because of the deprotonation of umbelliferone (umb). The pK_a of umb (7.11[35], 8[32]) is similar to the pK_a of *p*NP (7.1[36]) suggesting a similar reaction behaviour. During the reaction, the colour of the mixture gradually turned to a brown tone.

Although the TLC showed only a very fine new band after 2 h at 70 °C, the reaction mixture was further purified and gave a final yield of 7 %.

In view of this low yield, a time dependent reaction monitoring was performed using TLC after different time points. Since the intensity of the product band increased up to a total reaction time of 2 h and stagnated afterwards, all further reaction batches were heated for 2 h.

A new reaction was set up at 90 °C, but no product band was visible indicating that the product was either not formed or not stable at higher temperatures.

To avoid contaminating the reagents with water, TEA was distilled from CaH_2, and the solid reagents were dried over molecular sieves, but no significantly improved yield could be observed.

Interestingly, 3 – 5 equivalents of TEA (calculated by ^{1}H-NMR peak integration of different batches) were visible in the ^{1}H-NMR spectrum despite extensive co-evaporation with methanol. Due to the two phosphate groups in the ADPR derivatives, a maximum of only 2 equivalents of TEA as counterions is possible, indicating the presence of an inorganic salt since other additional peaks occurred neither in the ^{1}H-NMR nor in the ^{13}C-NMR. Hence, different solubility properties of the NAD^+ analogue with a protonated pyrophosphate moiety and of a potential inorganic salt could be used to purify ADPRumb.

To transfer the compound to the free acid form, the freeze-dried product was dissolved in a few drops of water and acidified to pH 2. After precipitation from ice-cold acetone[37], the clean ^{1}H-NMR showed only traces of the remaining TEA, indicating the successful conversion into the free acid form.

The characterisation of the compound was similar to the ADPR*p*NP with the challenge of poor solubility in water, but also in ethanol, hence giving small signals in the D_2O-NMR spectra.

The ^{13}C-NMR showed 21 out of 24 expected peaks, but fitting with the spectrum of ADPR*p*NP and the reference spectrum from the manufacturer of umb, Sigma-Aldrich. The configuration of the newly formed bond could not be determined due to the low intensity of the signals. Nevertheless, a similar reaction mechanism to the ADPR*p*NP synthesis suggested a β-configuration.

G.3) Biological testing and prerequisites

In this project, two potential chemical probes were synthesised and tested for their suitability for monitoring NAD^+ consuming enzymatic reactions.

Already existing enzyme testing conditions were adapted, using alternative substrates. If the native substrate NAD^+ was turned over under these conditions, the exchange of NAD^+ for the chemical probes would elucidate whether the alternative substrates were recognised.

As the cleavage product nicotinamide is neither colourimetrically nor fluorometrically measurable, a spectrophotometrically or fluorometrically detectable alternative enzymatic product would afford an elegant experimental setup. This implies the condition of selective measurement of the cleaved product only.

G.3.1) ADPR*p*NP on ADPR cyclase

Since ADPR cyclase from *Aplysia californica* has been used in the Wagner group before[38], the setup was adjusted to the following conditions: The reaction was performed in 50 mM HEPES buffer, pH 7.4, at 26 °C in a total enzyme concentration of 0.25 U/mL. Hence, each prerequisite experiment was conducted under these conditions.

G.3.1.1) Determination of a suitable wavelength

To selectively measure potentially cleaved *p*NP, an appropriate wavelength for the readout had to be found. Therefore, absorbance spectra of ADPR*p*NP and *p*NP were recorded in the same setting in which the enzyme experiment would be carried out.

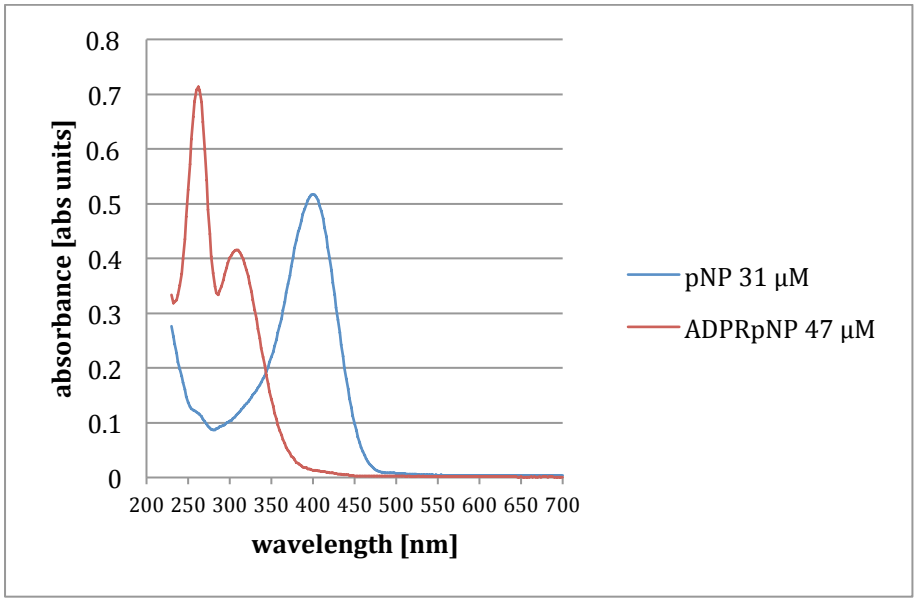

Figure 10: absorbance spectra of *p*NP and ADPR*p*NP at pH 7.4

Table 2: comparison of λ_{max} of *p*NP and ADPR*p*NP at pH 7.4

	λ_{max} [nm]	absorbance [abs units]
*p*NP 31 µM	400	0.517
ADPR*p*NP 47 µM	262	0.714
	308	0.416

Although the concentration of the two compared solutions were different, it was obvious that a wavelength near 400 nm would prove useful to selectively detect the cleavage product.

The aim of this experiment was not to determine the molar extinction coefficient, but only to establish a useful wavelength for absorbance assays. The closest available filter was 410 nm.

Table 3: absorbance values of *p*NP and ADPR*p*NP at pH 7.4

λ [nm]	absorbance [abs units]	
	*p*NP 31 µM	ADPR*p*NP 47µM
410	0.486	0.011

These findings suggested that absorbance measuring at 410 nm would be suited to selectively detect potential cleavage.

G.3.1.2) Calibration curve

In order to quantify a possible turnover by enzymatic activity, a calibration curve of *p*NP under the conditions of the enzyme experiment was needed.

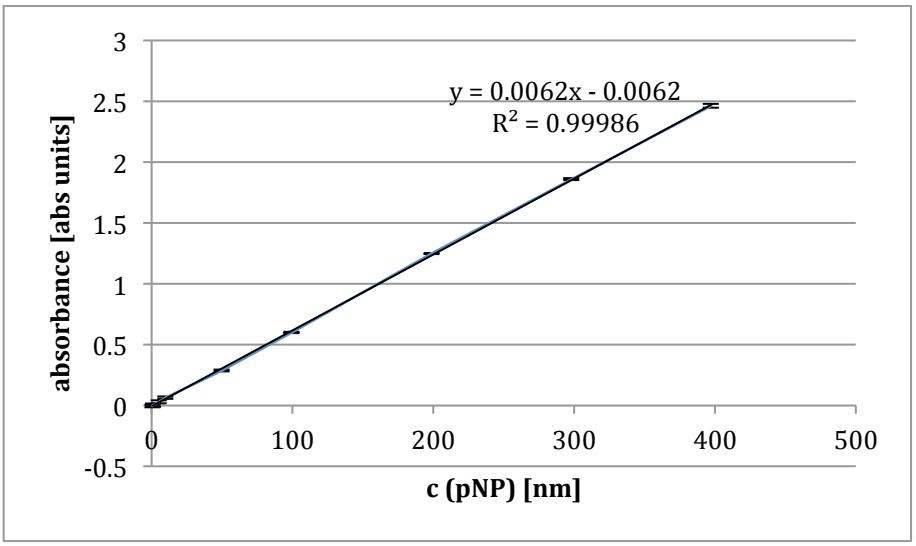

Figure 11: calibration curve of *p*NP using the absorbance at 410 nm at pH 7.4 (error indicating mean ± std of triplicates)

Different concentrations ranging from 0.5 µM to 5 mM were read out in triplicate. Figure 11 displays the average absorbance of each concentration within the best linearity range: 0.5 – 400 µM shows the highest coefficient of determination. When quantifying the absorbance values, no normalisation was chosen, resulting in a discrepancy between the measured absorbance at the spectrophotometer (0.486, see Table 3) when recording the spectrum and the calculated value from the linear regression (0.186, see Figure 11, when using the concentration of 31 µM). Since the readout of the enzyme experiment was performed in the same manner, the calibration curve was applicable.

G.3.1.3) Enzyme activity test

To qualitatively test the enzyme activity, ADPR cyclase was incubated with NAD^+ under the same conditions as the chemical probes: in 50 mM HEPES buffer, pH 7.4, at 26 °C. The reaction was monitored by TLC and compared with a negative control of buffer with NAD^+. Nicotinamide was used as a reference substance on the TLC plate.

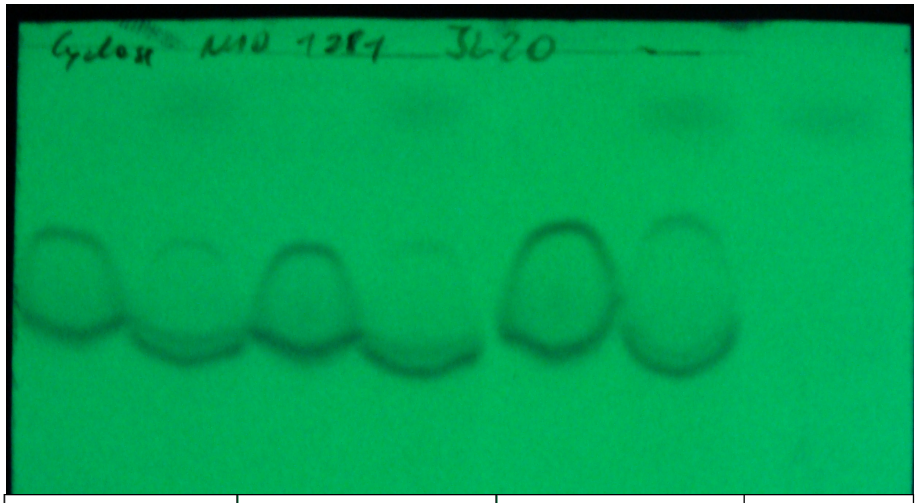

0 min		10 min		30 min		reference
+buf.	+enz.	+buf.	+enz.	+buf.	+enz.	nic.

Figure 12: ADPR cyclase activity test

NAD^+ was incubated with and without ADPR cyclase and samples were drawn after different time points. TLC plate under UV light (254 nm); buf., buffer; enz., enzyme; nic., nicotinamide

Figure 12 shows that nicotinamide (R_f 0.9) and at least one other product (R_f 0.3), according to the reaction scheme, cADPR and/or ADPR[39], were formed only in solutions containing enzyme, hence that ADPR cyclase was active. The high concentration of 1281 µM NAD^+ was chosen to be detectable by ultraviolet (UV) light on the TLC plate: the same experiment was performed using only 100 µM NAD^+, but the conversion was hardly visible under UV light (data not shown).

The results indicate that even at the first time point (here named 0 min, although there was a time interval of several seconds between combining the solutions and spotting the samples on the TLC) a cleavage took place, shown by the appearing nicotinamide spot at R_f 0.9. (In a separate TLC, it was shown that ADPR cyclase in buffer was clean, leading to the conclusion that the newly formed substances came from the enzymatic conversion of NAD^+.) The reaction was monitored up to 3 h, but the qualitative readout only by the naked eye could not give quantitative information about the progress of cleavage during the experiment.

The peculiar shape of the NAD^+ spots (two lines bent towards each other) could be explained by the very large diameter of the circles of spotted substance due to the use of Pasteur pipettes. Due to the similarity of the shapes of sample and negative control, it does not interfere with the validity of this test.

Moreover, the purpose of this experiment was not to distinguish between the different possible products (cADPR and linear ADPR). Instead, enzyme activity was correlated with formation of the cleaved product nicotinamide.

Although these results cannot provide quantitative information about the activity of ADPR cyclase, they confirm a basic, qualitative activity.

G.3.1.4) ADPRpNP on ADPR cyclase

Having shown that a suitable testing system was at hand, ADPR*p*NP was tested on ADPR cyclase. Different concentrations of ADPR*p*NP were mixed with enzyme solution and, as a negative control, with buffer only. A mixture of enzyme and buffer served as a blank and *p*NP in the same concentrations as ADPR*p*NP was used both as a positive control and as an on-plate calibration. The experiment was conducted in triplicate and monitored over 2 h, followed by another 2 h because no obvious change in absorbance could be seen.

To ensure homogeneity of the solutions in each well, a shaking period of 10 sec was added before the first readout.

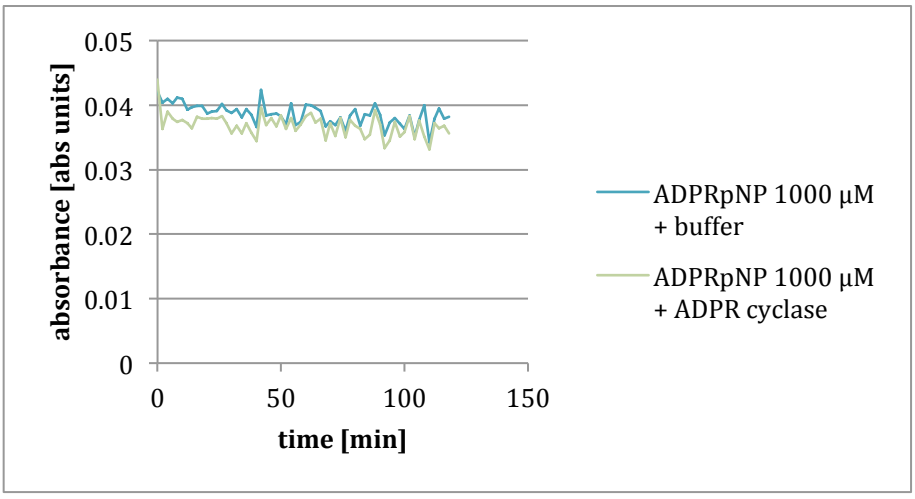

Figure 13: ADPR*p*NP on ADPR cyclase: comparison of highest concentration of ADPR*p*NP with and without enzyme

Figure 13 displays the effect of ADPR cyclase on ADPR*p*NP in the highest of all tested concentrations and emphasises that no time dependent change in absorbance could be detected. The lower concentrations showed similar results: no increase in absorbance due to

enzymatic cleavage. The small fluctuations are caused by the experiment noise and appear both with and without enzyme, thus having no influence on the validity of the experiment.

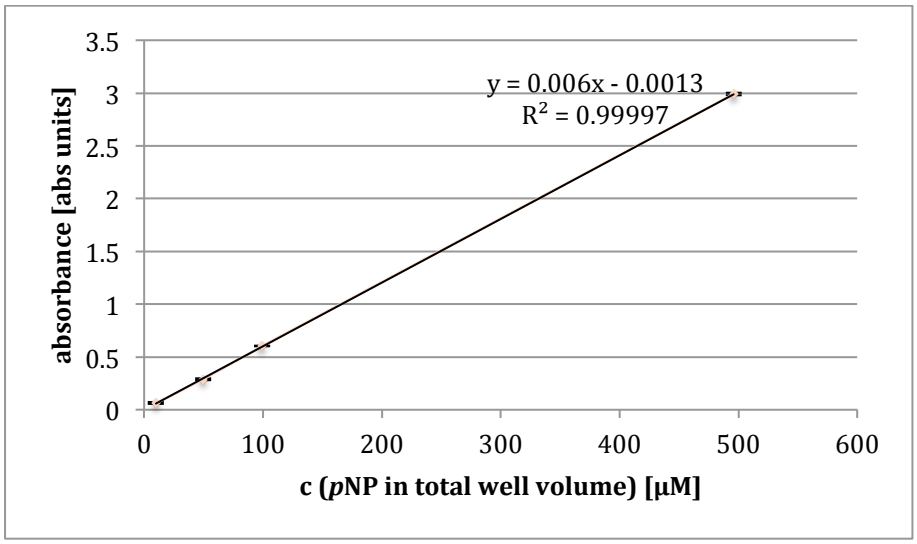

Figure 14: on-plate calibration curve of *p*NP (error indicating mean ± std of triplicates)

Due to the high linearity, the on-plate calibration curve (Figure 14) demonstrated a sensitively functioning readout setup.

One could argue that one triplicate with buffer only, serving as a blank, is necessary in this design, but missing. If the experiment had been repeated, this solution would have been included as a blank. Nevertheless, the comparison of the initial readout of the wells containing the same concentration of ADPR*p*NP, each, but either enzyme or buffer, showed that the enzyme did not influence the absorbance value significantly. This observation was supported by the relation between the absorbance of buffer only in the calibration experiment depicted in Figure 11, giving the value 0.116, and the absorbance of enzyme and buffer in the examination of ADPR*p*NP on cyclase, resulting in 0.118.

After 2 h, another measurement programme was added to read out the absorbance up to a total of 4 h, but no significant change could be noticed.
For this reason, ADPR*p*NP is not a substrate for ADPR cyclase of *Aplysia californica*.

G.3.2) ADPR*p*NP on NAD glycohydrolase

NAD glycohydrolase from porcine brain has previously been used in the Wagner group[38] and the system was adapted, resulting in the following conditions: The experiment was conducted in 50 mM Tris buffer, pH 8.0, at 37 °C in a total enzyme concentration of 0.0086 U/mL. Since NAD glycohydrolase is poorly soluble in Tris buffer, an endpoint readout of the supernatant of the reaction mixture was performed at 26 °C, a temperature convenient for the readout, but independent of the incubation process.

G.3.2.1) Determination of a suitable wavelength

Again, a suitable wavelength for selective cleavage detection had to be found, applying the readout conditions. Absorbance spectra of the potential substrate ADPR*p*NP and the possibly cleaved product *p*NP were recorded and compared.

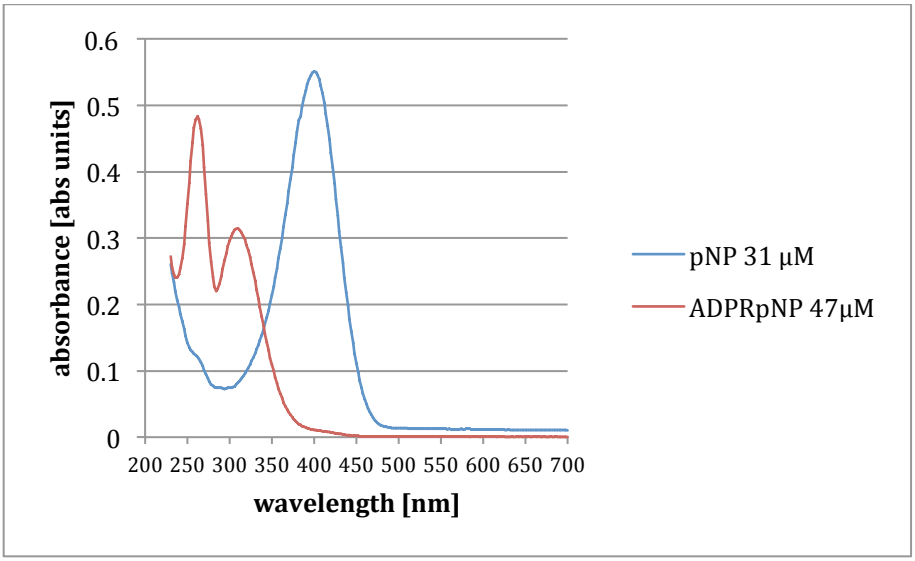

Figure 15: absorbance spectra of *p*NP and ADPR*p*NP at pH 8.0

Table 4: comparison of λ_{max} of *p*NP and ADPR*p*NP at pH 8.0

	λ_{max} [nm]	absorbance [abs units]
*p*NP 31 µM	400	0.550
ADPR*p*NP 47 µM	262	0.483
	310	0.314

Once more, the concentrations differed, but one could deduce that absorbance measurements at around 400 nm would lead to a selective readout. The nearest available filter was 410 nm, which was used henceforth.

Table 5: absorbance values at 410 nm

λ [nm]	absorbance [abs units]	
	*p*NP 31 µM	ADPR*p*NP 47 µM
410	0.518	0.009

G.3.2.2) Calibration curve

To quantify a possible turnover, a calibration curve was necessary. Different concentrations between 0.1 µM and 10 mM were tested, giving the best linearity in a range of 0.1 to 500 µM, which is depicted in Figure 16.

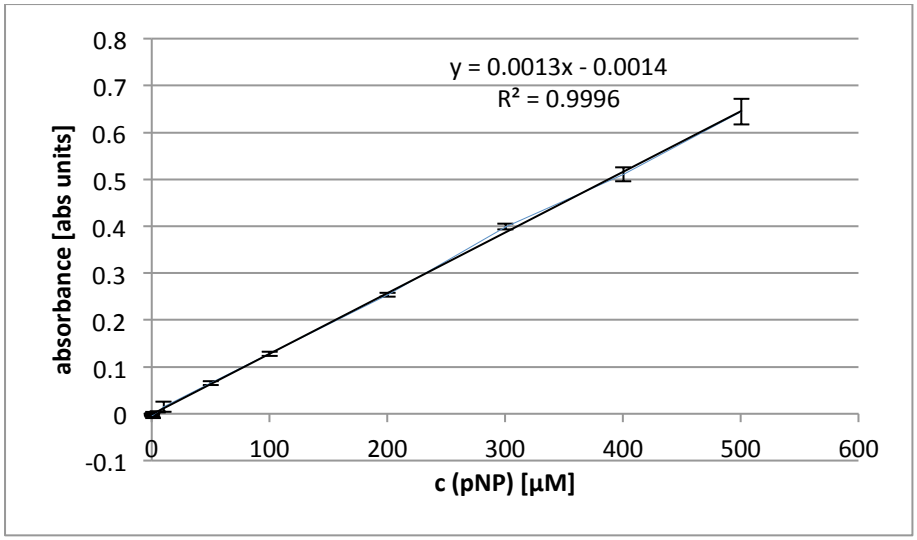

Figure 16: calibration curve of *p*NP using the absorbance at 410 nm at pH 8.0 (error bars represent mean ± std of triplicates)

Due to the fact that only 50 µL were pipetted in each well, the absorbance was distinctively different from the calibration curve in 200 µL HEPES buffer (see Figure 11).

G.3.2.3) NAD glycohydrolase activity test

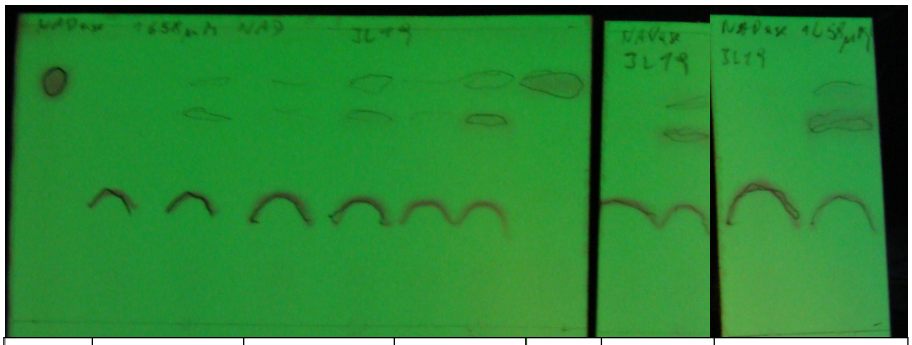

ref.	0 min		10 min		40 min		ref.	125 min		240 min	
nic.	+b	+e	+b	+e	+b	+e	nic.	+b	+e	+b	+e

Figure 17: NAD glycohydrolase activity test: TLC plate under UV light (254 nm)
ref., reference; nic., nicotinamide; b., buffer; e., enzyme

A solution of relatively high concentration of NAD^+ (1658 µM) was added to the enzyme and buffer solutions respectively to give a detectable spot on the TLC plate under UV light (254 nm) because the same experiment had been performed with only 100 µM NAD^+ before and the spots had only been vaguely visible (data not shown).

The weak spots in the negative control (NAD^+ + buffer) after 10 and 40 min are regarded as insignificant, especially when compared to the negative controls after 125 and 240 min, where no such spots are noticeable.

Even at the first time point (named 0 min, but in fact after a few minutes due to the experimental handling) a small fraction of NAD^+ was cleaved into nicotinamide (R_f 0.8) and another product (R_f 0.65), according to the reaction scheme, probably ADPR. The intensity of these spots increased time dependently, showing that even after 2 h, conversion was still taking place. A separate TLC confirmed the absence of NAD^+ and nicotinamide in the enzyme solution. Generally, turnover only took place in the presence of NAD glycohydrolase, confirming its activity.

G.3.2.4) ADPR*p*NP on NAD glycohydrolase

Since NAD glycohydrolase from porcine brain is poorly water soluble, a simple time dependent readout in a 96 well plate was not possible. Whereas other approaches involve solubilisation by either pancreas lipase or detergent[40], in this experiment a suspension was

used to incubate the enzyme with the potential substrate. Succeeding centrifugation gave a clear supernatant, which was used for the absorbance measurement.

After activation of the enzyme for 20 min at 37 °C, ADPR*p*NP was added in concentrations from 50 – 1000 µM. Samples were drawn after different time points and stored immediately on dry ice to stop any further reaction. After thawing, they were centrifuged to obtain a clear supernatant, which was then transferred to the plate.

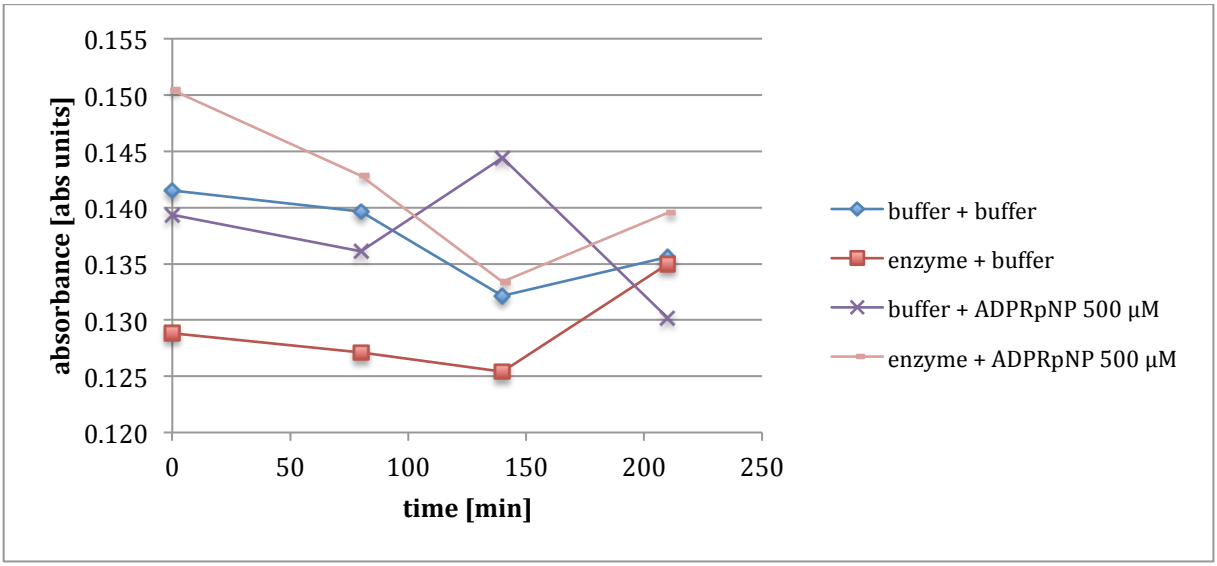

Figure 18: ADPR*p*NP on NAD glycohydrolase

Figure 18 shows the time dependent absorbance of ADPR*p*NP with and without enzyme, including solutions containing buffer only and enzyme only. The values were not blanked against any well to show that the different solutions gave similar readouts, which were close to the blank wells (buffer only) of the calibration curve of Figure 16, 0.146 ± 0.006.

Disadvantages of this method include the poor solubility of the enzyme. Even though special attention was paid to mixing suspensions before drawing samples, inhomogeneity remained an inherent problem. In addition, each time point constituted an individual well, as opposed to the continuous readout of the cyclase assay. Hence, small changes in absorbance could have been caused by pipetting errors.

No time dependent trend was detectable indicating that no selective cleavage took place.

Initially, this experiment was designed to give qualitative information whether ADPR*p*NP is a substrate for NAD glycohydrolase. If there had been any indications of significant cleavage, the setup would have been changed to a more precise, quantitative measurement.

Although the experiment was conducted only in singlicate and the data scattered considerably, one can deduce that ADPR*p*NP is not recognised by NAD glycohydrolase or at least turnover occurs only in an extent below the sensitivity level of the assay.

G.3.3) ADPRumb on ADPR cyclase

G.3.3.1) Determination of a suitable wavelength

To obtain a good readout, fluorescence properties had to be studied. Absorbance spectra were the first starting experiments for fluorescence recordings.

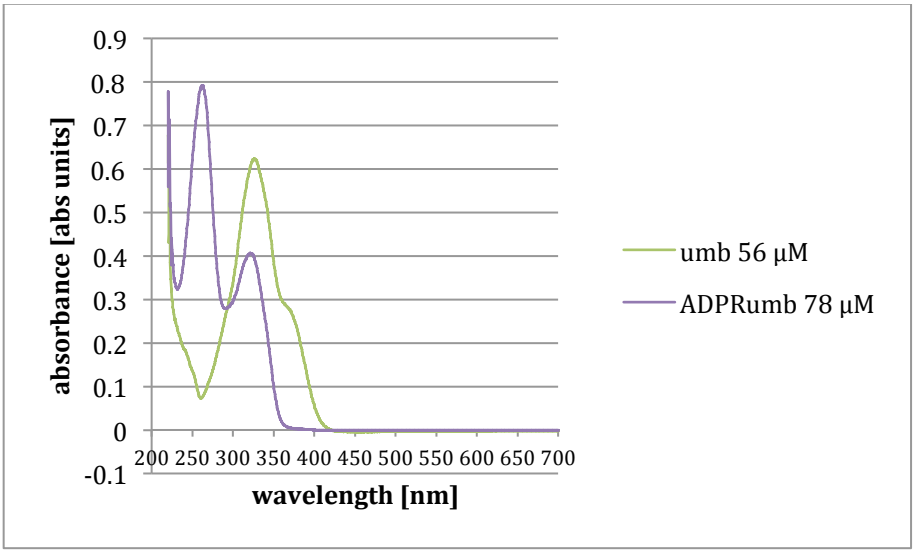

Figure 19: absorbance spectra of umb and ADPRumb at pH 7.4

Table 6: absorbance-λ_{max} of umb and ADPRumb at pH 7.4

	λ_{max} [nm]	absorbance [abs units]
umb 56 µM	326.5	0.624
ADPRumb 78 µM	262.5	0.791
	321.5	0.407

According to Table 6, excitation around 326.5 nm was likely to give a good fluorescence emission. To confirm that, 2D fluorescence spectra were recorded.

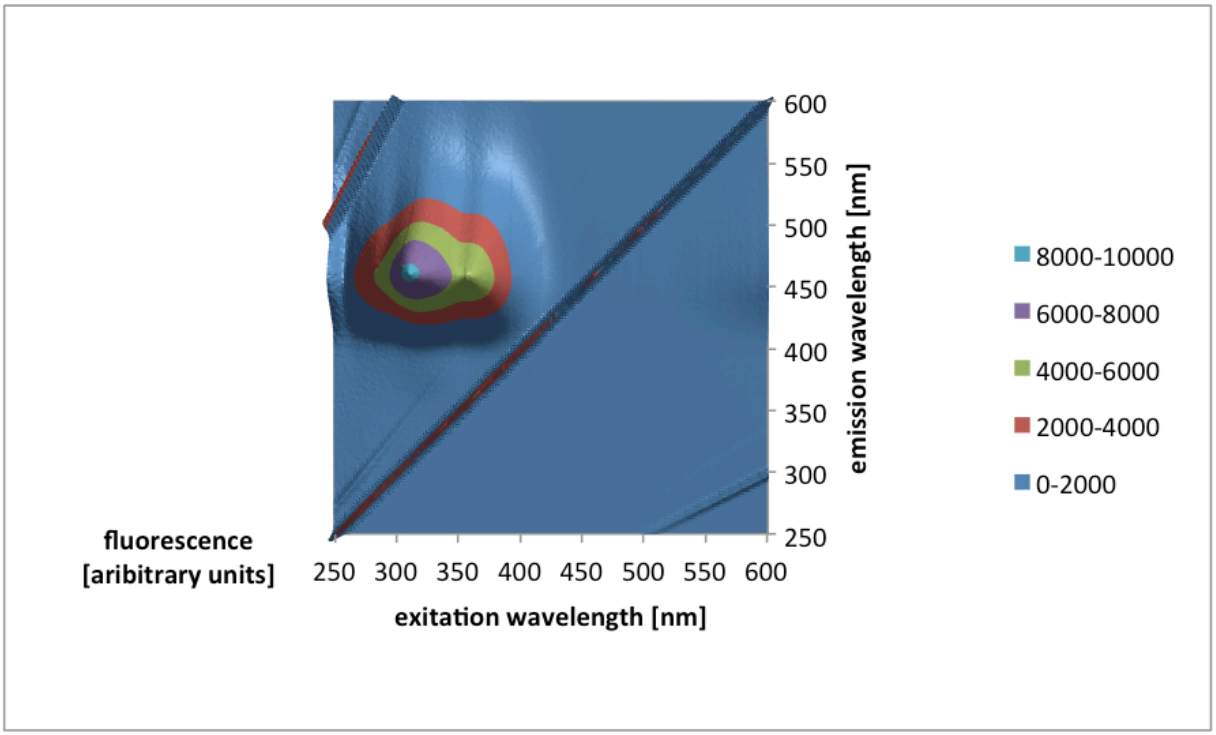

Figure 20: 2D fluorescence spectrum of umb 1.1 µM at pH 7.4

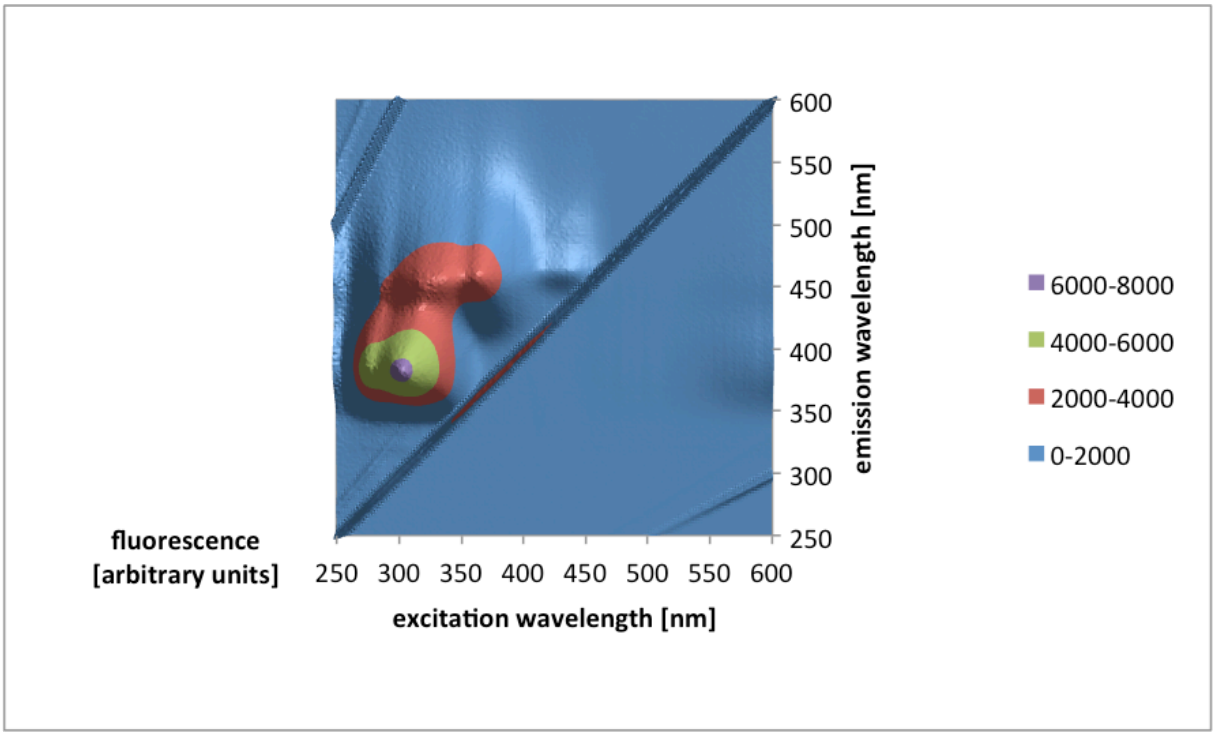

Figure 21: 2D fluorescence spectrum of ADPRumb 79 µM at pH 7.4

The linear features are the result of the Rayleigh Tyndall scatter, occurring when excitation wavelength equals, doubles or halves emission wavelength[41].

Table 7: fluorescence-λ_{max} of umb and ADPRumb at pH 7.4

λ_{max}	λ_{ex} [nm]	λ_{em} [nm]	fluorescence [arbitrary units]
umb 1.1 µM	328	456	8311
ADPRumb 79 µM	320	388	6312

The emission maximum of umb was measured at 456 nm, which made the available filter at 455 nm the best choice. To find out the best excitation wavelength, the data of the 2D fluorescence spectra of the two compounds were analysed with regard to the emission wavelength 456 nm to give Figure 22.

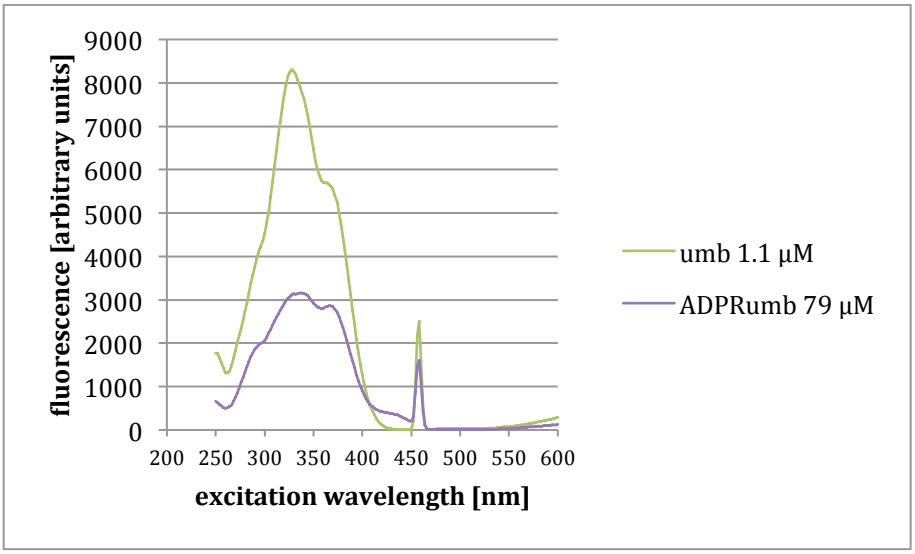

Figure 22: excitation spectra with emission wavelength fixed to 456 nm

Table 8: comparison of fluorescence using available excitation filters, emission filtered at 456 nm

λ_{ex} [nm]	fluorescence [arbitrary units]	
	umb 1.1 µM	ADPRumb 79 µM
320	7724	2912
350	6461	2924
410	445	541

Table 8 suggests that the excitation filter 320 nm would give the best selective readout for the release of umb.

G.3.3.2) Calibration curve

Concentrations from 5 nM – 50 µM were chosen to calculate a calibration curve in order to quantify a potential turnover of ADPRumb. Figure 23 shows the curve using the values of the best linearity (5 nM – 10 µM).

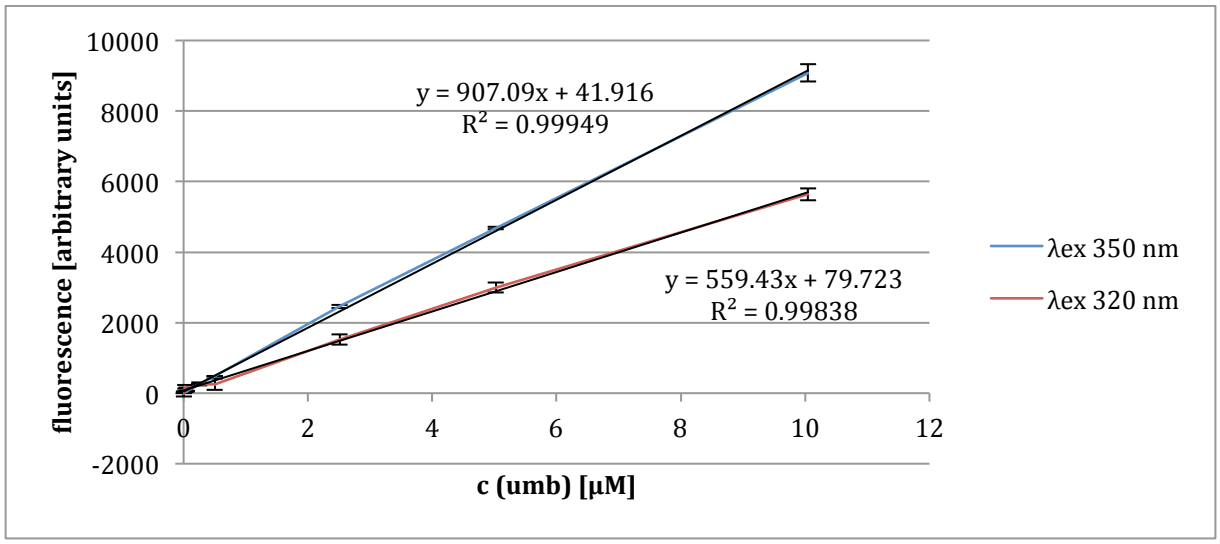

Figure 23: calibration curve of umb using the fluorescence emission at 455 nm at pH 7.4, comparing different excitation wavelengths (error bars show mean ± std of triplicates)

Intriguingly, a side experiment on the plate reader showed that a higher fluorescence could be obtained at the excitation wavelength of 350 nm, although Table 8 had predicted a lower readout. Hence, the calibration wells were read out at both excitation wavelengths (320 nm, 350 nm) and compared. Since the higher excitation wavelength gave a higher fluorescence and a higher coefficient of determination at the same instrument that would be used for enzymatic tests, 350 nm was selected as the excitation wavelength for future experiments.

G.3.3.3) ADPRumb on ADPR cyclase

Having determined all the required parameters for the testing system of the potential substrate and the enzyme, ADPRumb could be tested on *Aplysia* cyclase.

ADPRumb solutions were tested in a range of 5 to 1000 µM on both cyclase solution (total concentration 0.25 U/mL) and buffer as a negative control to show whether

hydrolysis occurred without enzyme. An on-plate calibration curve was performed using 0.5 to 50 µM umb solutions. The discrepancy between the concentrations of ADPRumb and umbelliferone were caused by the poor solubility of umb in buffer. Buffer only and enzyme only wells served as blanks and all combinations were performed in triplicate.
The reaction was monitored over 4 hours measuring the fluorescence every 3 min.
Additionally, the activity of the enzyme against the natural substrate NAD^+ was confirmed in the same setting using TLC before and after the reaction.

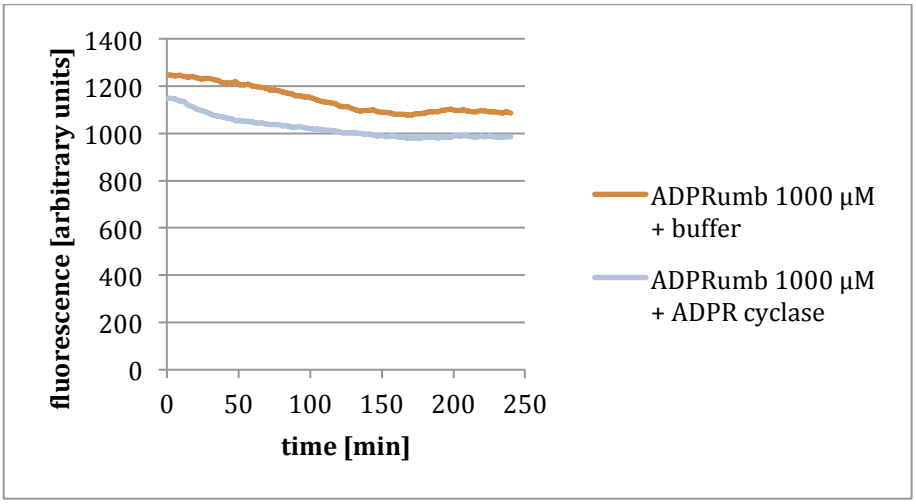

Figure 24: ADPRumb on ADPR cyclase

The comparison of ADPR solutions mixed with either buffer or enzyme would show a potential cleavage, in which case, an increase in fluorescence would be seen.
For reasons of clarity, Figure 24 only shows the highest tested concentration, which would display the highest fluorescence if cleaved, but it indicates that no such turnover took place.
On the contrary, a decrease in fluorescence over time could be observed but also in the umb wells, shown in Figure 25, suggesting photobleaching (i.e. photochemical destruction of the fluorophore), since substantial evaporation of fluorophore containing solution was unlikely at the reaction temperature of 26 °C.
The enzyme control experiment demonstrated an intact enzyme, which led to the conclusion that ADPRumb is not a substrate for *Aplysia* ADPR cyclase.

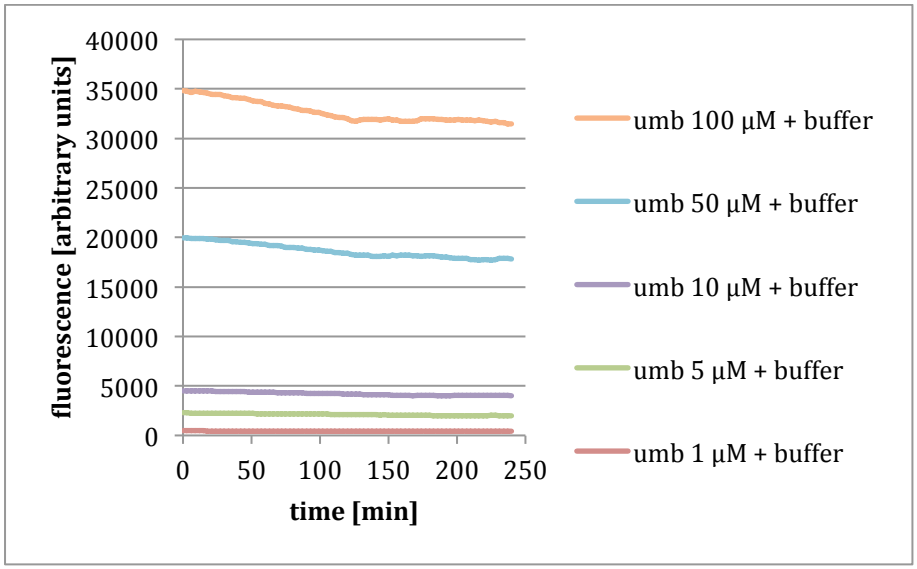

Figure 25: on-plate standards

G.3.4) ADPRumb on NAD glycohydrolase

G.3.4.1) Determination of a suitable wavelength

In order to find appropriate fluorescence conditions (excitation and emission wavelengths) to detect potential cleavage, absorbance spectra were recorded, firstly.

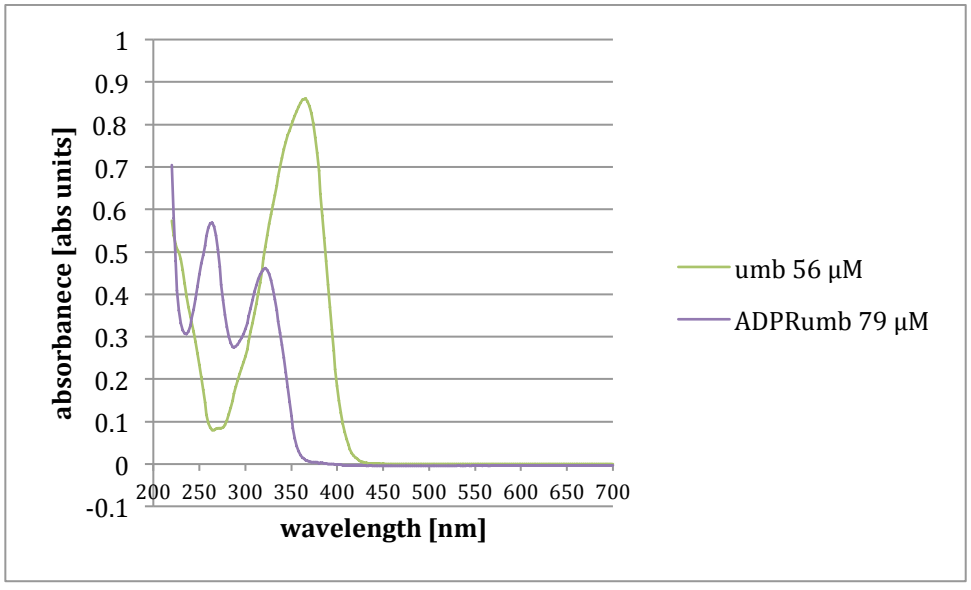

Figure 26: absorbance spectra of ADPRumb and umb at pH 8.0

Table 9: comparison of λ_{max} of umb and ADPRumb at pH 8.0

	λ_{max} [nm]	absorbance [abs units]
umb 56 µM	366	0.861
ADPRumb 79 µM	264	0.569
	322	0.461

According to Figure 26, a suitable excitation wavelength for a fluorescence experiment could be expected at around 366 nm. To confirm that and determine the ideal excitation wavelength, 2D fluorescence spectra were recorded and compared.

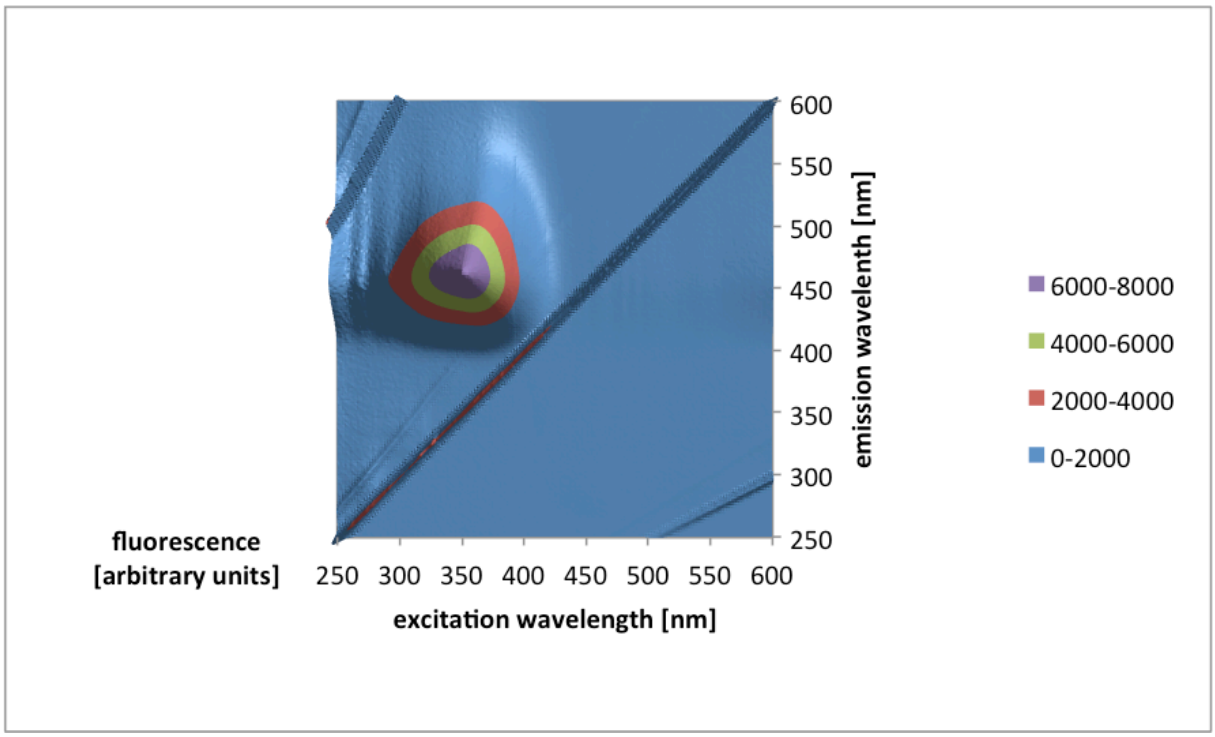

Figure 27: 2D fluorescence spectrum of umb 560 nM at pH 8.0

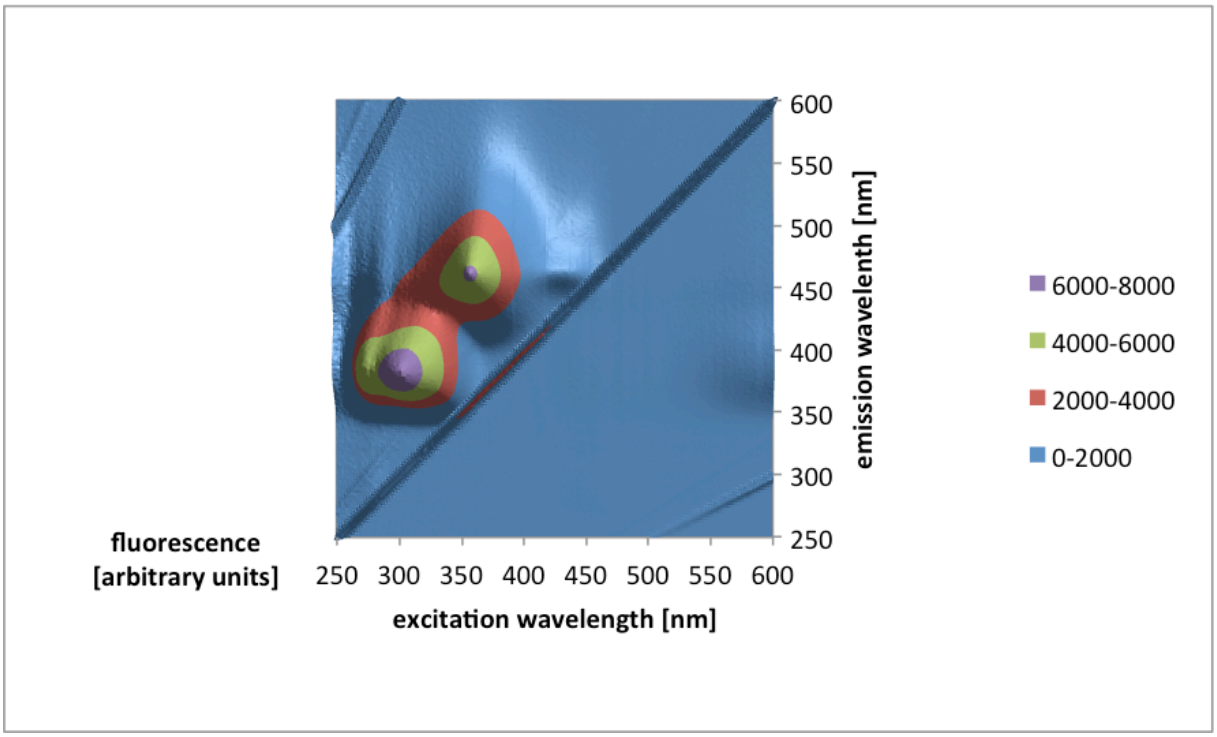

Figure 28: 2D fluorescence spectrum of ADPRumb 79 µM at pH 8.0

Table 10: λ_{max} of umb and ADPRumb at pH 8.0

λ_{max}	λ_{ex} [nm]	λ_{em} [nm]	fluorescence [arbitrary units]
umb 560 nM	364	456	7924
ADPRumb 79 µM	322	390	7096
	366	456	6186

The emission maximum of umb was measured as 456 nm, which made the available filter at 455 nm the best choice. To find out the best excitation wavelength, the data of the 2D fluorescence spectra of the two compounds were analysed with regard to the emission wavelength 456 nm to give Figure 29.

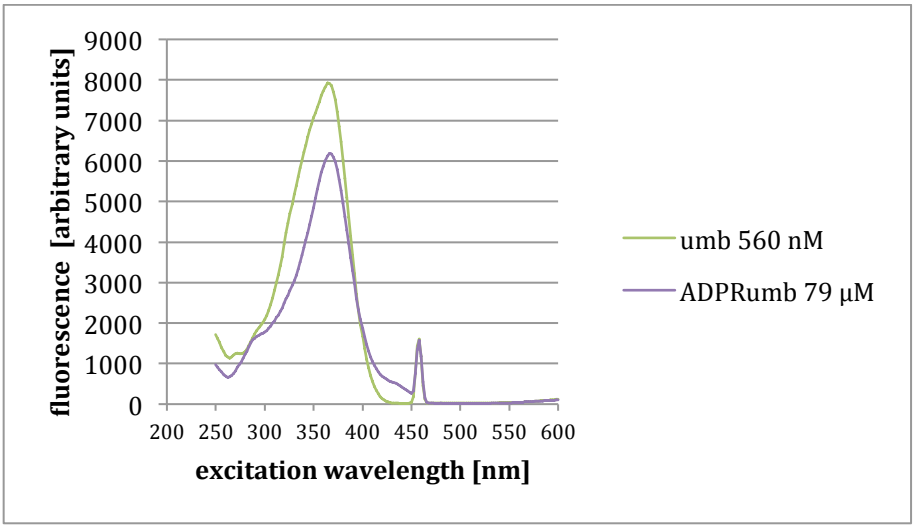

Figure 29: Excitation spectra of umb and ADPRumb with emission wavelength fixed to 456 nm

Applying the possible excitation wavelengths of the plate reader to this data set lead to Table 11.

Table 11: comparison of fluorescence of umb and ADPRumb using available excitation filters, emission filtered at 456 nm

	fluorescence [arbitrary units]	
λ_{ex} [nm]	umb 560 nM	ADPRumb 79 µM
320	3948	2494
350	7079	4848
410	563	1061

The fact that two different concentrations were chosen to give a suitable signal for the 2D spectra makes direct comparison more complicated. Assuming applicability of Beer–Lambert law, one can still draw valid conclusions. The high fluorescence of umb at excitation wavelength 350 nm despite the low concentration compared to ADPRumb (suggesting a high quantum yield, although not calculated) makes this setting the most promising.

G.3.4.2) Calibration curve

To be able to quantify a potential cleavage, a calibration curve of umb in Tris buffer was created. Concentrations between 1 nM and 60 µM were measured, giving the best linearity between 1 nM and 20 µM as depicted in Figure 30.

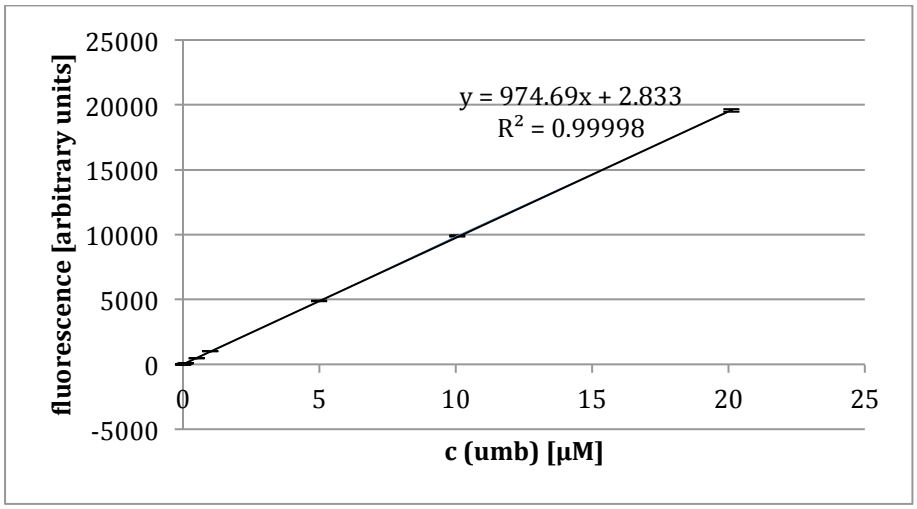

Figure 30: calibration curve of umb using the fluorescence excitation at 350 nm and emission at 455 nm at pH 8.0 (error bars show mean ± std of triplicates)

G.3.4.3) ADPRumb on NAD glycohydrolase

Having a suitable fluorescence system and a calibration curve at hand, the effect of NAD glycohydrolase on ADPRumb was examined. Using the same enzymatic setup as with ADPR*p*NP, fluorescence of reaction solutions after 0, 70, 145 and 240 min was measured. Figure 31 shows the values after correction against buffer and enzyme, if applicable.

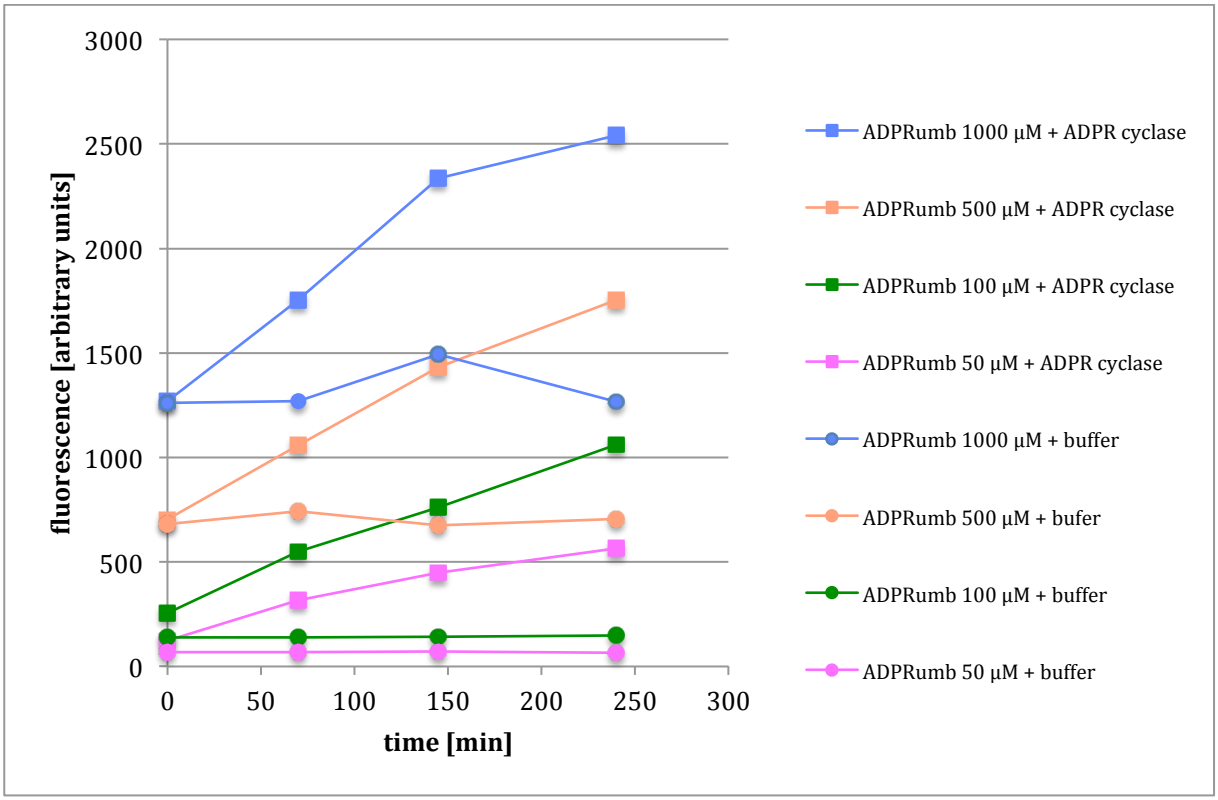

Figure 31: ADPRumb on NAD glycohydrolase

Table 12 shows the fraction of cleaved umb from ADPRumb, calculated according to the regression equation from Figure 30, indicating that ADPRumb is only a weak substrate for NAD glycohydrolase. The inverse relation between concentration of substrate and fraction of split ADPRumb (see Figure 32) fits the enzymological theory. Due to the experimental setup, detailed kinetics could not be analysed. In light of the poor turnover, even after 4 hours, it did not seem worth investing time and effort.

The numbers given in Table 12 should be interpreted considering that the experiment was conducted only in singlicate. This implies the notion that the measured value of one experiment is not the mean of a bigger sample and would have to be corrected after several repeats of the experiment.

Moreover, the small turnover numbers of the low concentrations of substrate at time point 0 min could be explained by both the experimental delay between adding the enzyme and the first measurement, and the experimental scatter due to potential pipetting errors. Nevertheless, a general trend was observable and it can be stated that ADPRumb is only a weak substrate for NAD glycohydrolase.

Table 12: turnover of ADPRumb in the presence of NAD glycohydrolase

turnover (%)		time [min]			
		0	70	145	240
c (ADPRumb) of added solution [µM]	1000	0.00%	0.11%	0.20%	0.30%
	500	0.01%	0.15%	0.36%	0.50%
	100	0.27%	0.98%	1.47%	2.18%
	50	0.24%	1.18%	1.80%	2.38%

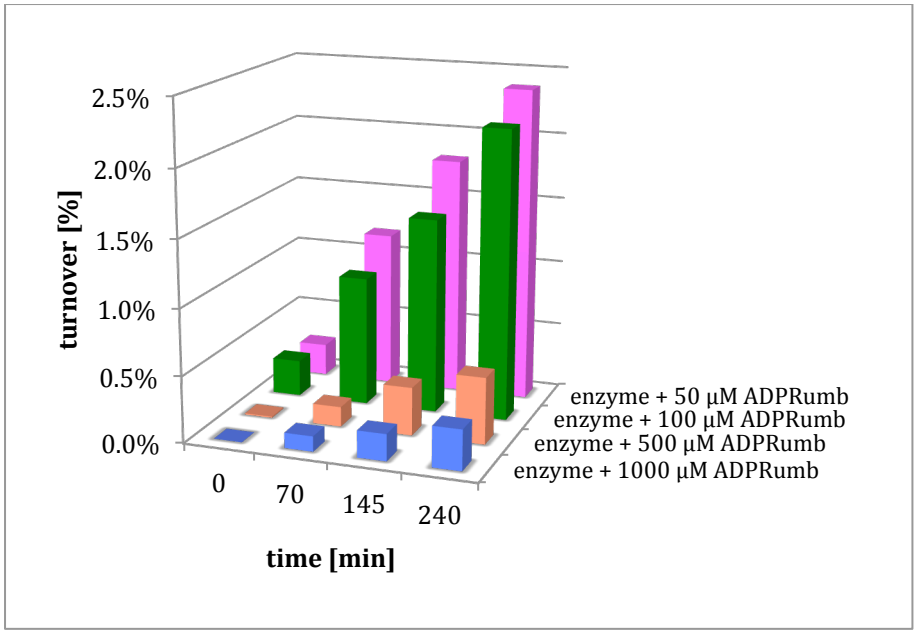

Figure 32: turnover of ADPRumb in the presence of NAD glycohydrolase

H) Summary and Outlook

NAD^+ consuming enzymes have been gaining attention over the last years and have been shown to play fundamental roles in cell regulation. Especially, their involvement in disease and lifespan has prompted research to investigate their molecular mechanisms and to screen for modulators. In this work, two molecules have been synthesised, characterised and tested on their suitability to act as chemical probes to visualise the enzymatic activity of two NAD^+ consuming enzymes.

In this project, ADPR*p*NP, an already known colorigenic substrate for some NAD^+ consuming enzymes, was synthesised and described using various NMR techniques. After achieving appropriate absorbance settings and enzyme conditions, ADPR*p*NP was tested on ADPR cyclase from *Aplysia californica* and NAD glycohydrolase from porcine brain. However, in neither case turnover could be detected, suggesting that ADPR*p*NP is not useful to probe these enzymes.

The synthetic strategy was adapted to form ADPRumb, a compound unreported before, designed to act as a fluorogenic substrate. After characterising the molecule and determining an applicable fluorescence setup, ADPRumb was studied on the previously mentioned enzymes, ADPR cyclase and NAD glycohydrolase. Whereas the cyclase exhibited no turnover, NAD glycohydrolase could be shown to cleave the substrate, resulting in an increase in fluorescence, though very slowly.

This work presents the synthesis of a known compound, ADPR*p*NP and extends the range of enzymes, on which it has been tested as a chemical probe, albeit negatively. Furthermore, it shows the synthesis of a new compound, ADPRumb, and the tests for its suitability as a chemical probe on two enzymes. On NAD glycohydrolase from porcine brain, it showed a turnover too low to make use of ADPRumb as a chemical probe.

This project provides a basis for future work in the field of NAD^+ analogues with exchanged nicotinamide moiety. The synthetic route would benefit from improving the yield, either through a different synthetic avenue or modifying the existing one after a more systematic

analysis of parameters influencing the yield: temperature, time, solvent, pH, ratio of amounts of reagents, securing anhydrous conditions and separation technique.

Extension of the applicability of the presented molecules as chemical probes on other enzymes could prove useful. Especially, clinically more relevant enzymes, such as sirtuins, PARPs or the human ADPR cyclase CD38, constitute interesting potential targets of chemical probes.

I) Experimental Section

I.1) General instruments and methods

Column Chromatography

Preparative chromatography was carried out on a BioLogic LP chromatography system equipped with a proportioning valve and mixer module, a controller a 254 nm UV optics module, a conductivity cell and a fraction collector. The following methods were used:

Method a: Ion pair chromatography was conducted on a system comprising LiChroprep RP-18 (25 – 40 µm) resin as stationary phase and gradient of methanol against 0.05 M triethylammonium bicarbonate (TEAB) buffer pH 7.4.

Method b: Anion exchange chromatography was performed on two BioScale Mini Macro-Prep High Q Cartridges, 5 mL each, attached consecutively, using a variable gradient of 1 M TEAB buffer pH 7.4 against MilliQ H_2O.

In either case, fractions were spotted on a TLC plate and eluated. Compound containing fractions were merged and evaporated to dryness.

Absorbance and Fluorescence Spectroscopy

To record the absorbance spectra, samples were transferred to a quartz micro cuvette (light path 10 x 4 mm) and measured on a Perkin Elmer Lambda 2 UV/Vis spectrometer at room temperature.

Fluorescence spectra were recorded on a Jasco FP-8200 fluorescence Spectrometer in a quartz micro fluorescence cuvette (light path 10 x 4 mm) at room temperature.

Absorbance and Fluorescence Plate Reader

Absorbance and fluorescence readouts were conducted in a BMG Labitech POLARstar OPTIMA microplate reader. The absorbance was measured in transparent Nunc MicroWell Plates with Nunclon Delta Surface, whereas fluorescence measurements were performed in Thermo Scientific Nunc F96 MicroWell Plates.

Thin Layer Chromatography

TLC was performed on TLC silica gel 60 F_{254} aluminium sheet using an eluent mixture of isopropanol: 0.2 % NH_4OH (7:3). The substances were detected under UV-light, 254 nm and 365 nm (Mineralight Lamp UVGL-58).

Mass Spectrometry

Accurate electrospray ionization mass spectra were obtained on a Finnigan MAT 900 XLT mass spectrometer at the EPSRC National Mass Spectrometry Service Centre, Swansea.

Nuclear Magnetic Resonance Spectrometry

NMR spectra were recorded at 298 K on Bruker BioSpin GmbH. ^{1}H-NMR spectra were recorded at 400 MHz, ^{13}C-NMR spectra were recorded at 101 MHz and ^{31}P-NMR spectra were recorded at 162 MHz. Chemicals shifts (δ) are reported in ppm (parts per million) and coupling constants (J) in Hz. Splitting patterns are abbreviated as follows: s: singlet, d: doublet, t: triplet, q: quartet, m: multiplet.

The water peak was set to 4.79 ppm[42].

Chemicals

All chemicals were obtained commercially and used as received unless stated otherwise. For the preparation of ADPRumb, TEA was distilled from CaH_2 and stored in an airtight flask. ADPR cyclase from *Aplysia californica* was purchased from Sigma-Aldrich and stock solutions thereof (50 U/mL) were prepared in HEPES buffer (50 mM, pH 7.4) and stored at -20 °C.

I.2) Synthesis and purification of ADPRpNP

Adenosine diphosphate ribose *p*-nitrophenol[31]

Chemical Formula: $C_{21}H_{26}N_6O_{16}P_2$

Molecular Weight: 680.41 g/mol

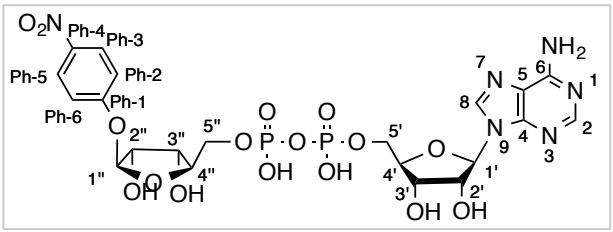

Figure 33: ADPR*p*NP

β-NAD^+ (100 mg, 0.151 mmol, 1 eq), *p*NP (105 mg, 0.755 mmol, 5 eq) and NaBr (622 mg, 6.04 mmol, 40 eq) were mixed with 1 mL anhydrous DMSO in a round bottom flask under an atmosphere of N_2. To this mixture was added 50 µL TEA. While stirring, the reaction was heated to 70°C and, after 2 h under N_2-atmosphere, was allowed to cool to room temperature. The excess of DMSO was removed by rotary evaporation and subsequent freeze-drying.

The product was purified by reversed-phase chromatography (0 – 40 % methanol against 0.05 M TEAB over 300 mL, flow rate: 1 mL/min, fraction size: 3 mL) followed by an ion-exchange chromatography (0 – 100 % 1 M TEAB against water over 300 mL, flow rate: 2 ml/min, fraction size: 5 mL). To further purify, another reversed-phase chromatography (settings as stated above) was performed. After removing the excess of TEAB by co-evaporation with methanol and freeze-drying, the slightly yellow product was obtained in 13 % yield (18 mg, 20 µmol, 0.13 eq, 2.3 eq TEA as determined by NMR).

^{1}H-NMR spectrum

(400 MHz, D_2O) δ 8.35 (s, 1H, H-8), 8.01 (s, 1H, H-2), 7.91 (d, *J* = 9.3 Hz, 2H, H-Ph-3, H-Ph-5), 6.91 (d, *J* = 9.3 Hz, 2H, H-Ph-2, H-Ph-6), 6.00 (d, *J* = 5.9 Hz, 1H, H-1'), 5.66 (d, *J* = 4.5 Hz, 1H, H-1''), 4.63 (t, *J* = 5.5 Hz, 1H, H-2'), 4.49 – 4.43 (m, 1H, H-3'), 4.41 (dd, *J* = 6.0, 4.7 Hz, 1H, H-2''), 4.39 – 4.32 (m, 2H, H-4', H-4''), 4.27 (dd, *J* = 6.1, 2.7 Hz 1H, H-3''), 4.22 (s, 2H, H-5'a, H-5'b), 4.13 – 4.02 (m, 2H, H-5''a, H-5''b), 3.32 (s, 0H, Methanol), 3.16 (q, *J* = 7.3 Hz, 13H, CH_2 TEA), 1.24 (t, *J* = 7.3 Hz, 20H, CH_3 TEA).

^{13}C-NMR spectrum

(101 MHz, D_2O) δ 161.64, 155.13, 152.48 (C-2), 148.52, 141.36, 139.42 (C-8), 125.43 (C-Ph-3, C-Ph-5), 116.11 (C-Ph-2, C-Ph-6), 100.24 (C-1''), 86.68 (C-1'), 84.58 (C-4''), 83.73 (C-4'), 74.41 (C-2'), 71.16 (C-2''), 70.25 (C-3'), 69.62 (C-3''), 65.61 (C-5''), 65.20 (C-5'), 46.56 (CH_2 TEA), 8.14 (CH_3 TEA).

^{31}P-NMR spectrum

(162 MHz, D_2O) δ -11.11 – -11.63 (m).

Mass spectrum

m/z (ESI) 679.0784 $[M-H]^-$, $C_{21}H_{25}N_6O_{16}P_2^-$ requires 679.0808

339.0358 $[M-2H]^{2-}$, $C_{21}H_{24}N_6O_{16}P_2^-$ requires 339.0367

TLC

Isopropanol: 0.2 % NH_4OH (7:3) R_f 0.78

I.3) Synthesis and purification of ADPRumb

Adenosine diphosphate ribose umbelliferone

Chemical Formula: $C_{24}H_{27}N_5O_{16}P_2$

Molecular Weight: 703.45 g/mol

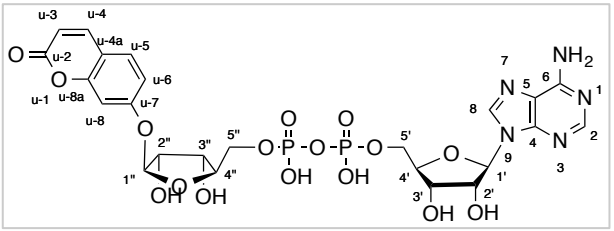

Figure 34: ADPRumb

β-NAD^+ (100 mg, 0.151 mmol, 1 eq), umb (122 mg, 0.755 mmol, 5 eq) and NaBr (622 mg, 6.04 mmol, 40 eq) were mixed with 1 mL anhydrous DMSO in a round bottom flask under an atmosphere of N_2. To this mixture was added 50 µL freshly distilled TEA. While stirring, the reaction was heated to 70 °C and, after 2 h under N_2-atmosphere, was allowed to cool to room temperature. The excess of DMSO was removed by rotary evaporation and subsequent freeze-drying.

The product was purified by reversed-phase chromatography (0 – 40 % methanol against 0.05 M TEAB buffer over 300 mL, flow rate: 1 mL/min, fraction size: 4 mL) followed by an ion-exchange chromatography (0 – 100 % 1 M TEAB against water over 300 mL, flow rate: 2

ml/min, fraction size: 5 mL). To further purify, another reversed-phase chromatography (settings as stated above) was performed. After removing the excess of TEAB by co-evaporation with methanol and freeze-drying, the product was obtained in 7 % yield (12 mg, 10 µmol, 0.07 eq, 5 eq TEA as determined by NMR).

The compound was dissolved in a few drops of water and acidified with 0.5 % aqueous HNO_3 to pH 2. After the addition of ice-cold acetone, the suspension was centrifuged and the supernatant discarded. The pellet was evaporated to dryness and freeze-dried to obtain the compound with a yield of 4 % (4 mg, 6 µmol, 0.04 eq).

^{1}H-NMR spectrum

(400 MHz, D_2O) δ 8.37 (s, 1H, H-8), 8.07 (s, 1H, H-2), 7.80 (d, *J* = 9.4 Hz, 1H, H-u-4), 7.33 (d, *J* = 8.6 Hz, 1H, H-u-5), 6.87 (d, *J* = 8.6 Hz, 1H, H-u-6), 6.76 (s, 1H, H-u-8), 6.27 (d, *J* = 9.5 Hz, 1H, H-u-3), 5.99 (d, *J* = 5.2 Hz, 1H, H-1'), 5.72 (d, *J* = 4.2 Hz, 1H, H-1''), 4.61 (t, *J* = 5.1 Hz, 1H, H-2'), 4.49 – 4.36 (m, 4H, H-3', H-2'', H-4'', H-4'), 4.32 – 4.24 (m, 3H, H-3'', H-5'a, H-5'b), 4.21 – 4.14 (m, 1H, H-5''a), 4.13 – 4.05 (m, 1H, H-5''b).

^{13}C-NMR spectrum

(101 MHz, D_2O) δ 164.17 (C-u), 159.45 (C-u), 154.04 (C-u), 149.07 (C-2), 145.45 (C-u-4), 129.22 (C-u-5), 123.04 (C-Adenine), 114.46 (C-u-6), 113.50 (C-u), 112.44 (C-u-3), 103.28 (C-u-8), 100.40 (C-1''), 87.51 (C-1'), 84.36 (C-4''), 83.61 (C-4'), 74.57 (C-2'), 71.16 (C-2''), 70.16 (C-3'), 69.61 (C-3''), 65.80 (C-5''), 65.18 (C-5').

^{31}P-NMR spectrum

(162 MHz, D_2O) δ -11.19 (d, *J* = 20.8 Hz), -11.42 (d, *J* = 20.3 Hz)

TLC

Isopropanol: 0.2 % NH_4OH (7:3) R_f 0.83

Mass spectrum

m/z (ESI) 702.0844 $[M-H]^-$, $C_{24}H_{26}N_5O_{16}P_2^-$ requires 702.0855

I.4) ADPR*p*NP on ADPR cyclase and prerequisites

The pH of aqueous HEPES buffer was adjusted to pH 7.4 with 1 M NaOH and filled up with water to a total concentration of 50 mM.

ADPR*p*NP on ADPR cyclase

The assay was carried out on a 96 well plate, using 50 mM HEPES buffer at pH 7.4 as a solvent. 100 µL ADPR*p*NP solution (20, 100, 200 and 1000 µM) was added to 100 µL cyclase solution (0.5 U/mL). As a negative control, the enzyme was omitted and buffer was used instead. *p*NP in the same concentrations as ADPR*p*NP served as an on-plate calibration curve. A mixture of 100 µL enzyme solution and 100 µL buffer was used as a blank. Each combination was performed in triplicate.

After 10 sec of shaking (4 mm, 150 rpm, double orbital), the absorbance at 410 nm at 26 °C was read out using 20 flashes per well. The absorbance was recorded every 2 min to a total of 120 min.

Calibration curve of *p*NP at pH 7.4

200 µL of each concentration in 50 mM HEPES buffer at pH 7.4 was pipetted on a 96 well plate in triplicate. The absorbance was measured at 410 nm at 26 °C, using the average of 20 flashes per well. The values were corrected against pure 50 mM HEPES buffer at pH 7.4.

ADPR cyclase activity test

50 mM HEPES buffer at pH 7.4 was used as a solvent. 100 µL cyclase solution (0.5 U/mL) was added to 100 µL NAD^+ solution (1280 µM and 100 µM respectively) on a 96 well plate. Mixtures of 100 µl buffer and each of the 100 µL NAD^+ solutions served as negative controls. The experiment was conducted at 26 °C in the plate reader. To monitor the turnover of NAD^+, samples were drawn after various time points up to 180 min. The samples, the negative controls, as well as nicotinamide as a standard were spotted on a TLC plate and eluted by isopropanol: 0.2 % NH_4OH (7:3).

I.5) ADPRumb on ADPR cyclase and prerequisites

The assay was performed on a black 96 well plate, using 50 mM HEPES buffer pH 7.4 as a solvent. ADPRumb solutions were prepared at concentrations of 5, 10, 50, 100, 500, 1000 µM. 100 µL of these solutions were mixed with either 100 µL of 0.5 U/mL cyclase solution or 100 µL of buffer. An on-plate calibration was carried out with 200 µL of umb solutions in concentrations of 0.5, 2.5, 5, 25, 50 µM. Enzyme only and buffer only wells served as blanks. All combinations were performed in triplicate and read out after initial shaking (4 mm, 150 rpm, double orbital) for 10 sec at 26 °C on a plate reader (excitation 350 nm, emission 455 nm, gain 1000, 20 flashes/well). The fluorescence was recorded every 3 min up to 240 min.
The enzyme control test included 100 µL NAD^+ solution (1000 µM) mixed with either 100 µL enzyme solution or 100 µL buffer. TLC was spotted before inserting in the plate reader and afterwards. Nicotinamide (500 µM) was used as a reference substance. TLC system: isopropanol: 0.2 % NH_4OH (7:3)

Calibration curve of umb at pH 7.4

The calibration curve was performed on a black 96 well plate using 50 mM HEPES buffer, pH 7.4, as a solvent.
The fluorescence (excitation 350 nm, emission 455 nm, gain 1000, 20 flashes/well) of 200 µL of each concentration was measured at 26 °C. The experiment was performed in triplicate and blanked against buffer.

ADPR cyclase activity test

See “ADPR*p*NP on ADPR cyclase and prerequisites”

I.6) ADPR*p*NP on NAD glycohydrolase and prerequisites

The pH of aqueous Tris buffer was adjusted to pH 8.0 with 1 M HCl and filled up with water to a total concentration of 50 mM.

ADPR*p*NP on NAD glycohydrolase

5 eppendorf tubes were filled with 200 µL suspension of 0.015 U/mL NAD glycohydrolase in Tris buffer each and placed on a dry block heater at 37 °C. After 20 min, to every tube was added 150 µL ADPR*p*NP solution (1000, 500, 100, 50 µM, respectively) and in one tube 150 µL of buffer serving as a control. Samples of 75 µL were drawn at different time points and stored immediately on dry ice for at least 15 min. After letting them thaw, the samples were centrifuged at 10,000 rpm for 5 min. 50 µL of each supernatant was transferred to a transparent 96 well plate and the absorbance was read out at 410 nm at 26 °C. A blank, consisting of 350 µL buffer, was treated in the same way. Mixtures of 200 µL buffer and 150 µL ADPR*p*NP solution at each concentration served as controls.

Calibration curve of *p*NP at pH 8.0

50 µL of each concentration in 50 mM Tris buffer at pH 8.0 was pipetted on a 96 well plate in triplicate. The absorbance was measured at 410 nm at 26 °C, using the average of 20 flashes per well. The values were corrected against pure 50 mM Tris buffer at pH 8.0.

NAD glycohydrolase activity test

2 eppendorf tubes of 200 µL suspension of 0.015 U/mL NAD glycohydrolase in Tris buffer each were put on a dry block heater at 37 °C. After 20 min, 150 µL NAD^+ solution (1660 and 100 µM, respectively) were added to the enzyme suspensions. Samples were drawn after several time points up to 240 min and spotted on a TLC plate besides the standard substance nicotinamide. The TLC was conducted in a system of isopropanol: 0.2 % NH_4OH (7:3).
Negative controls were performed using buffer only instead of enzyme.

I.7) ADPRumb on NAD glycohydrolase and prerequisites

5 eppendorf tubes were filled with 200 µL suspension of 0.021 U/mL NAD glycohydrolase in Tris buffer each and placed on a dry block heater at 37 °C. After 20 min, to every tube was added 150 µL ADPRumb solution (1000, 500, 100, 50 µM, respectively) and in one tube 150 µL of buffer serving as a control. Samples of 75 µL were drawn at different time points and stored immediately on dry ice for at least 15 min. After letting them thaw, the samples were centrifuged at 10,000 rpm for 5 min. 50 µL of each supernatant was transferred to a black 96

well plate and the fluorescence readings (excitation 350 nm, emission 455 nm, gain 1250, orbital averaging: 3 mm diameter) were taken at 26 °C, using the average of 15 flashes per well. A blank, consisting of 350 µL buffer, was treated in the same way. Mixtures of 200 µL buffer and 150 µL ADPRumb solution at each concentration served as controls. A positive enzyme activity control was performed using a mixture of 200 µL NAD glycohydrolase suspension and 150 µL 1000 µM NAD^+ solution and a negative one using 200 µL buffer with 150 µL 1000 µM NAD^+ solution. After the same workup as the other mixtures, the enzyme activity controls were run on a TLC using isopropanol: 0.2 % NH_4OH (7:3) and nicotinamide as a standard substance.

Calibration curve of umb at pH 8.0

50 µL of each concentration in 50 mM Tris buffer at pH 8.0 was pipetted on a black 96 well plate in triplicate. The fluorescence (excitation 350 nm, emission 455nm, gain 1250, orbital averaging: 3 mm diameter) was measured at 26 °C, using the average of 15 flashes per well. The values were corrected against pure 50 mM Tris buffer at pH 8.0.

J) NMR and mass spectra

J.1) ADPR*p*NP

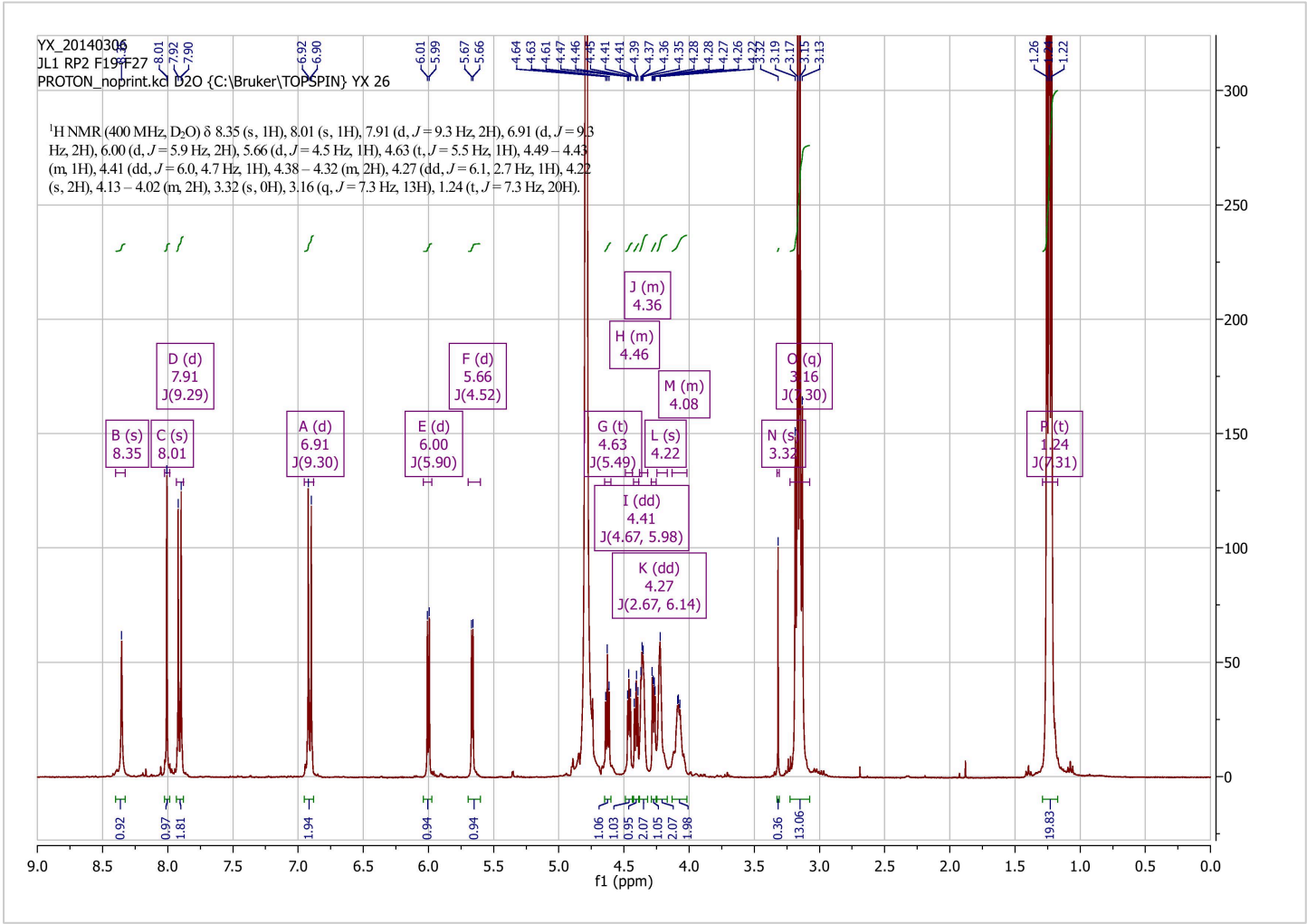

Figure 35: ^{1}H-NMR spectrum of ADPR*p*NP

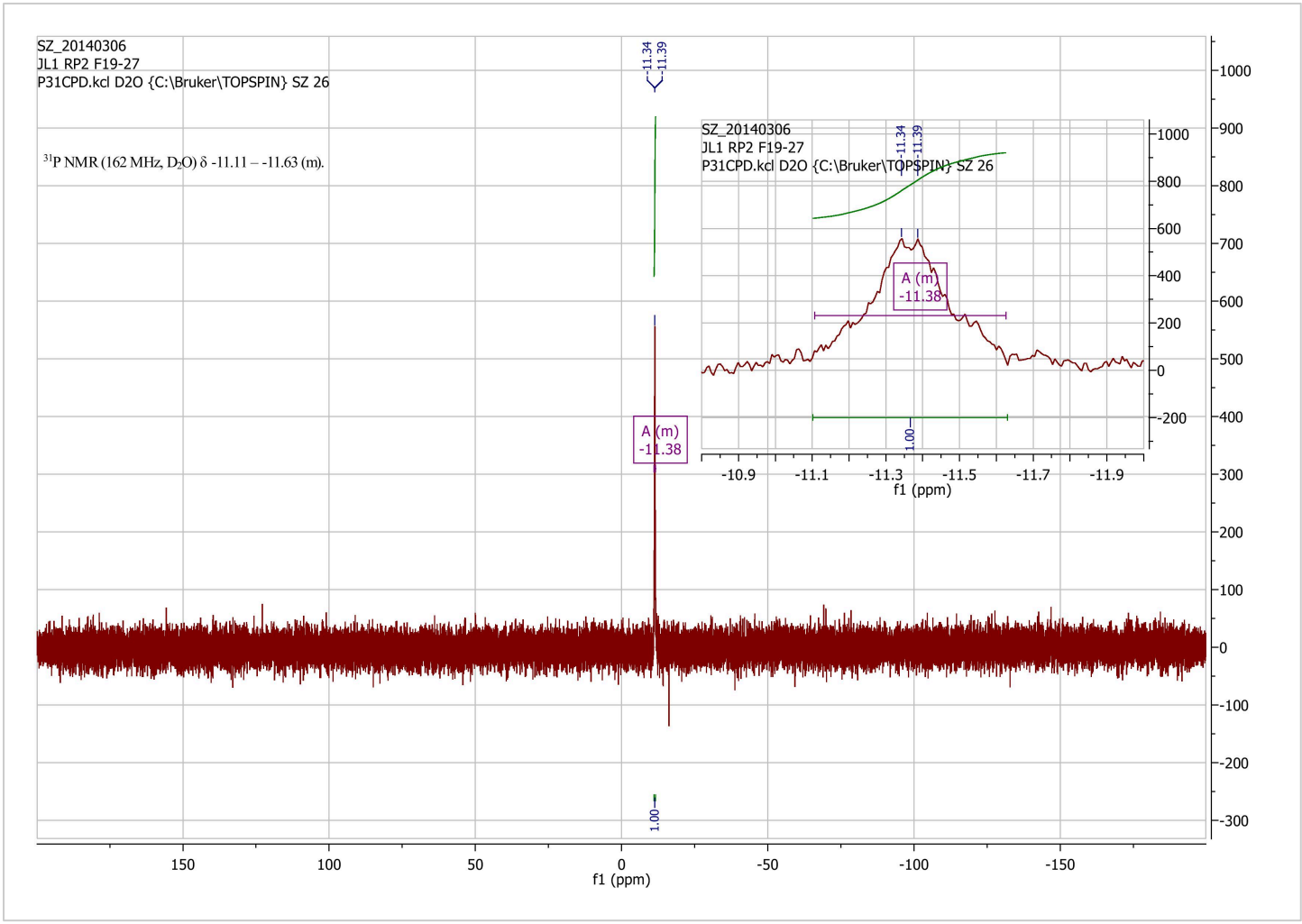

Figure 36: ^{31}P-NMR spectrum of ADPR*p*NP

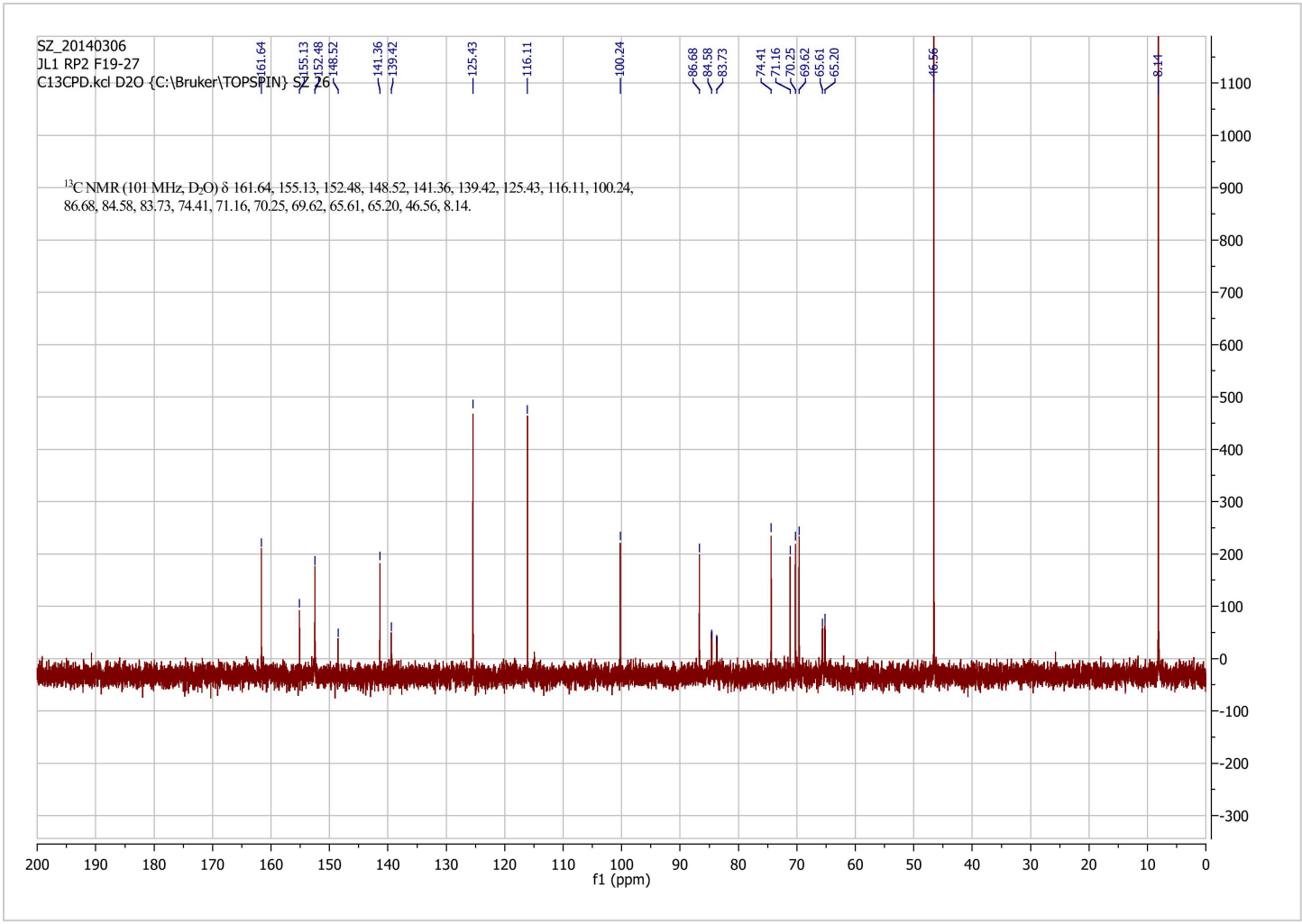

Figure 37: ^{13}C-NMR spectrum of ADPR*p*NP

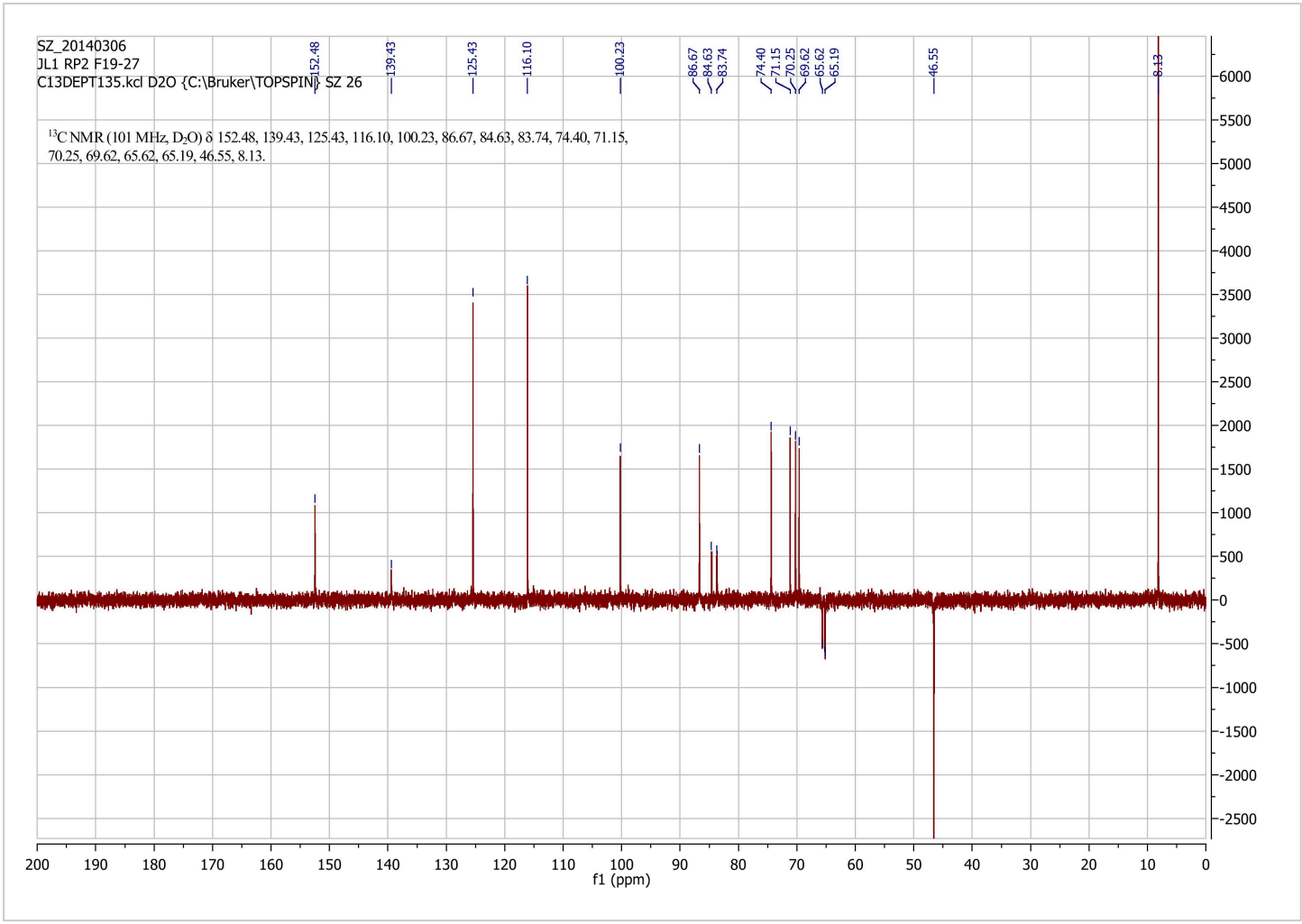

Figure 38: DEPT135 spectrum of ADPR*p*NP

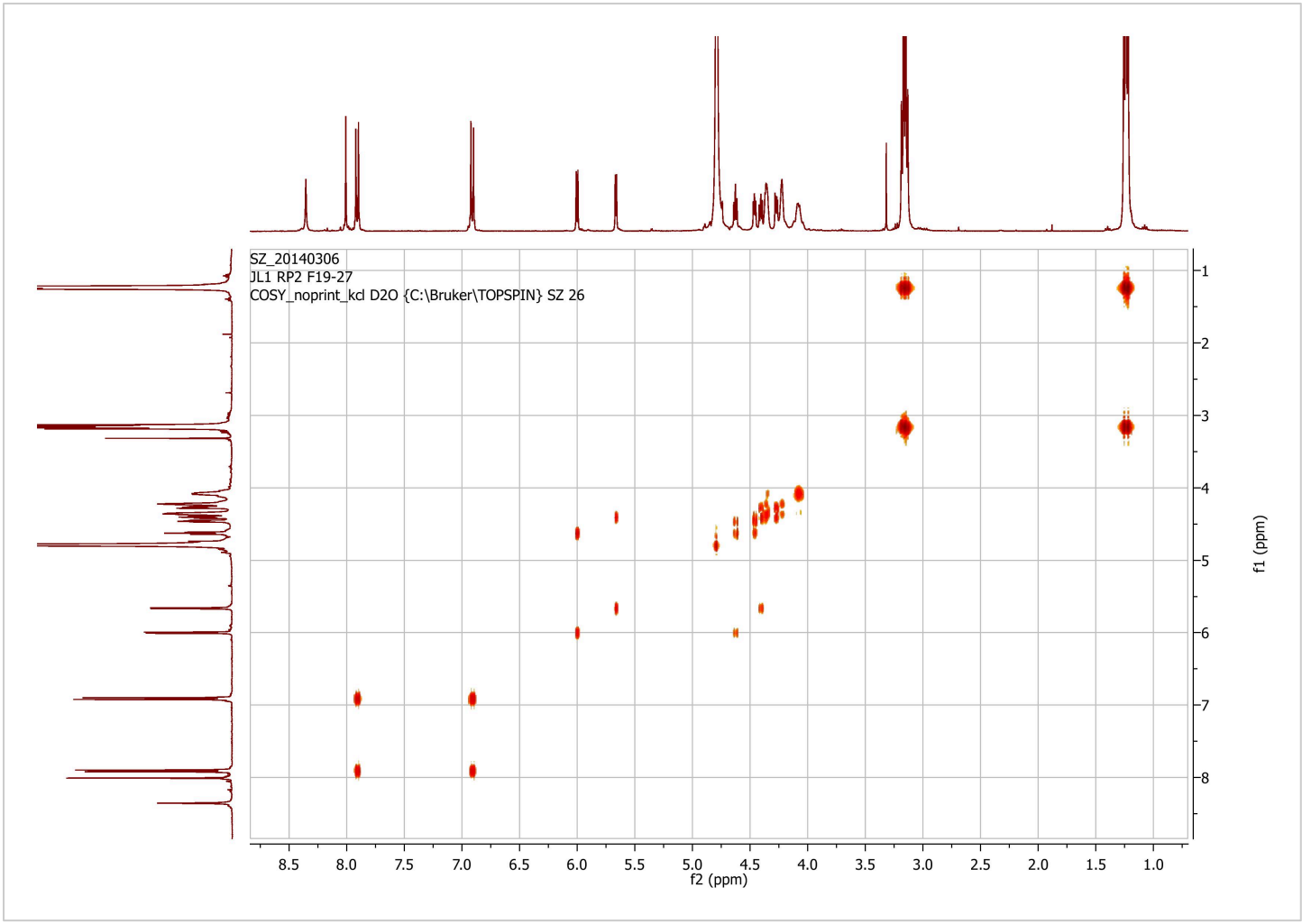

Figure 39: COSY spectrum of ADPR*p*NP

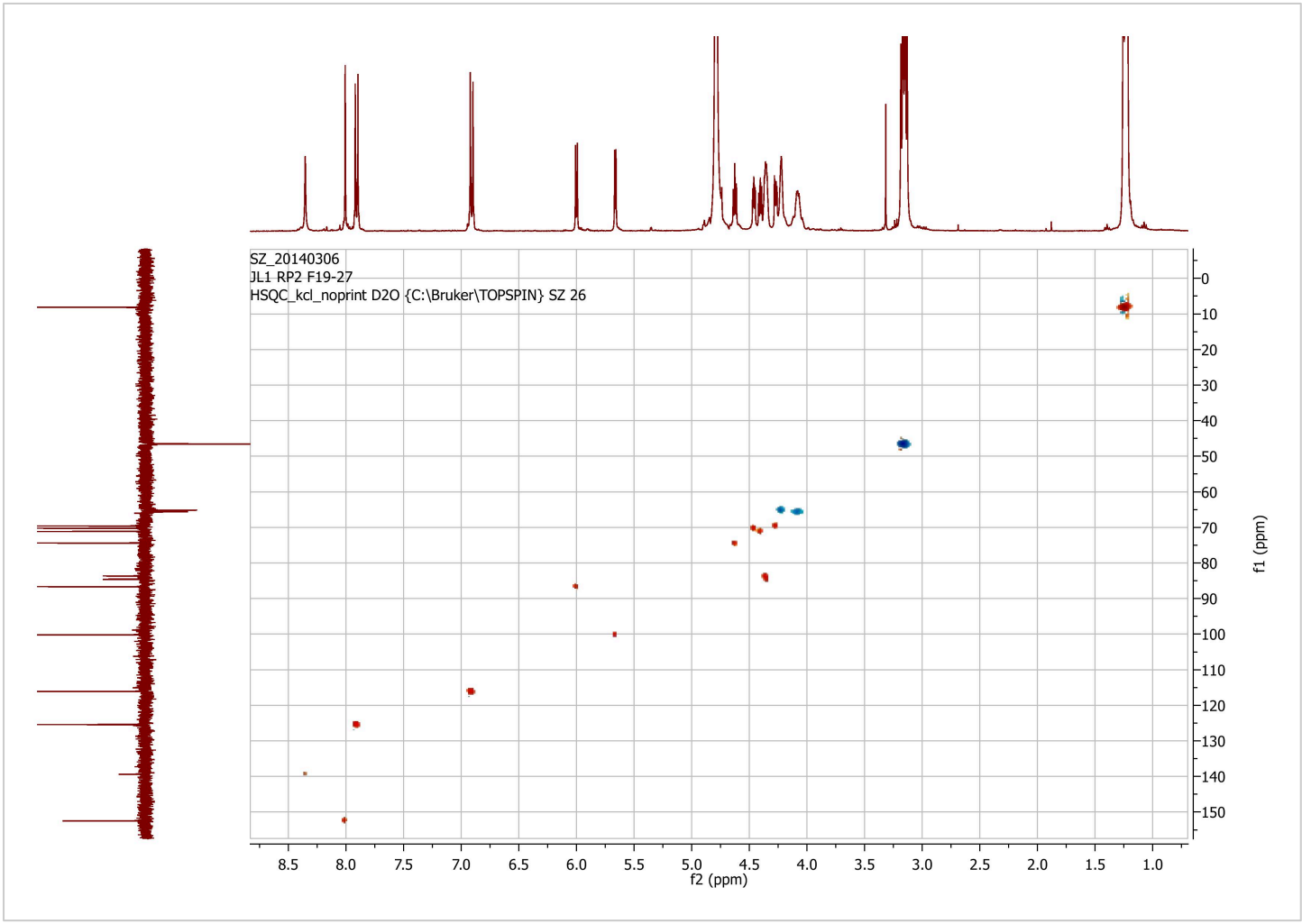

Figure 40: HSQC spectrum of ADPR*p*NP

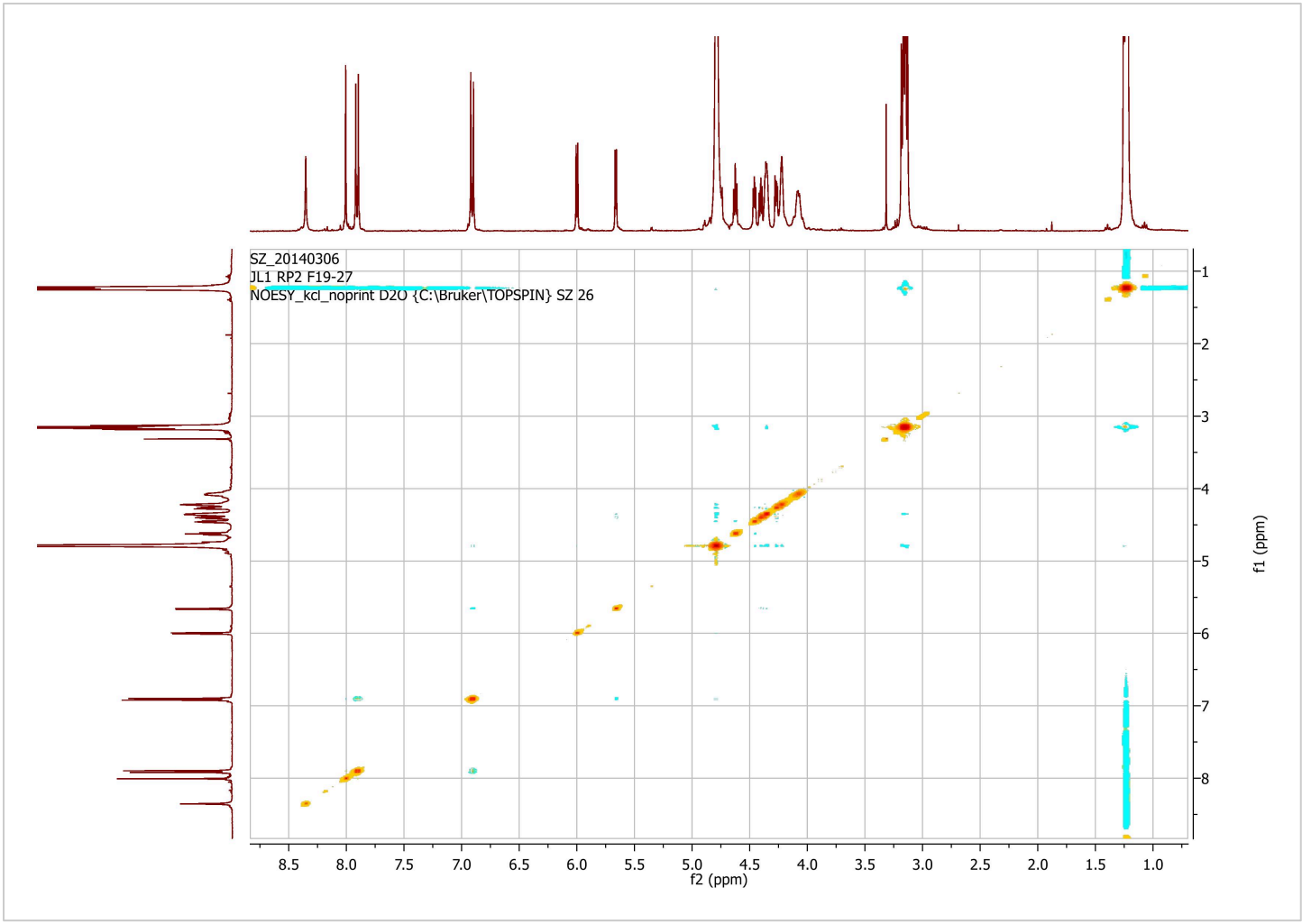

Figure 41: NOESY spectrum of ADPR*p*NP

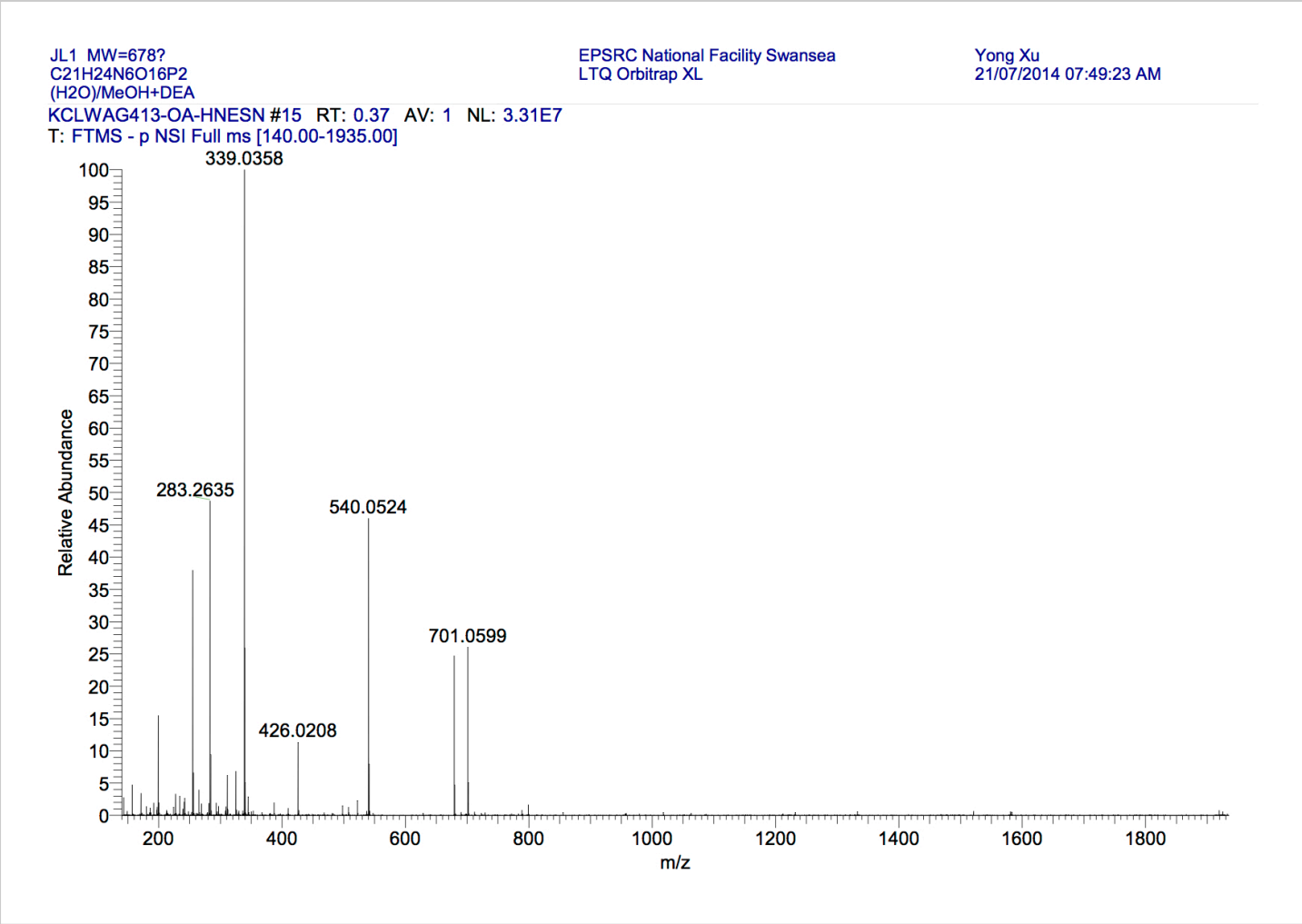

Figure 42: mass spectrum of ADPR*p*NP

J.2) ADPRumb

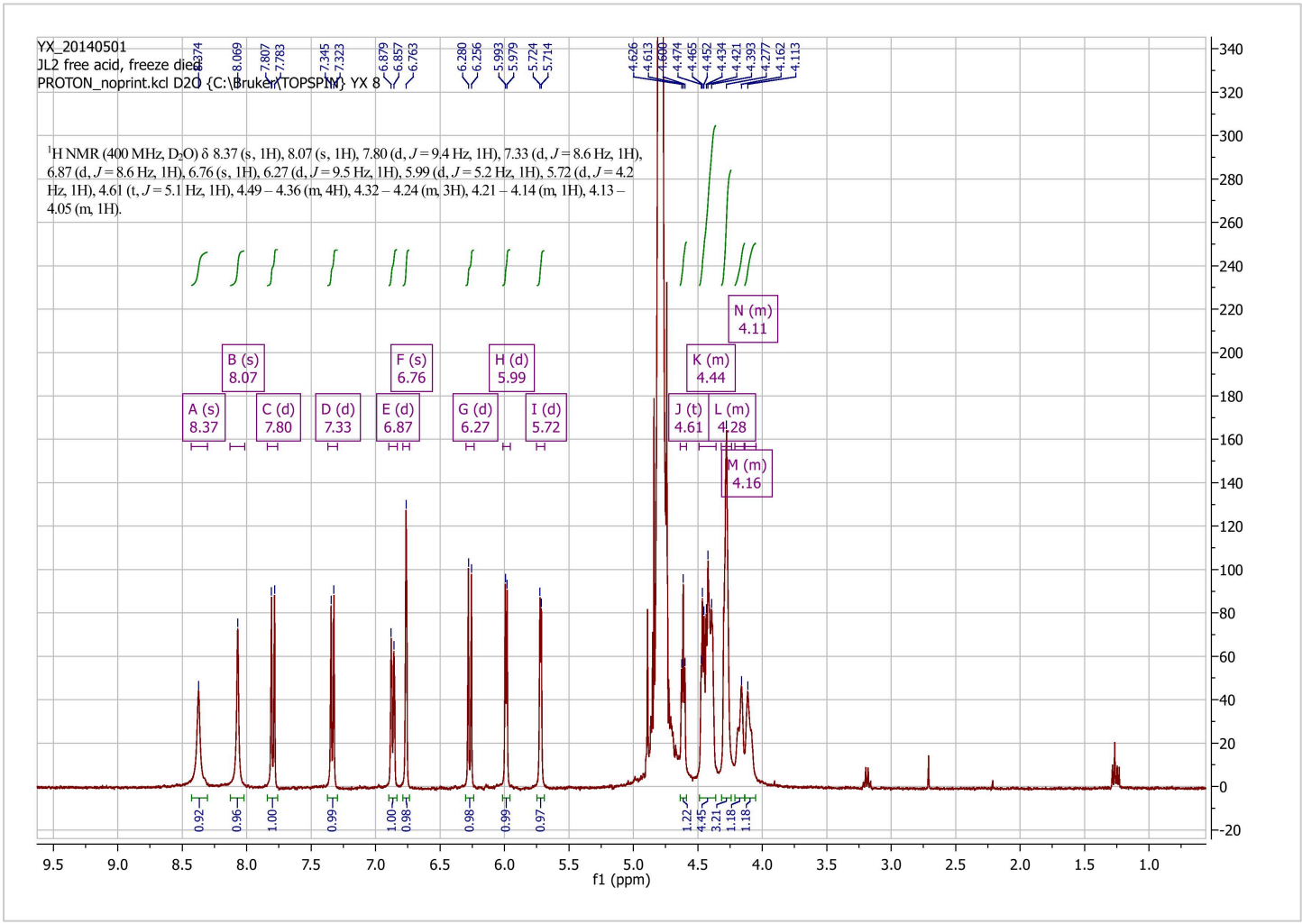

Figure 43: ^{1}H-NMR spectrum of ADPRumb

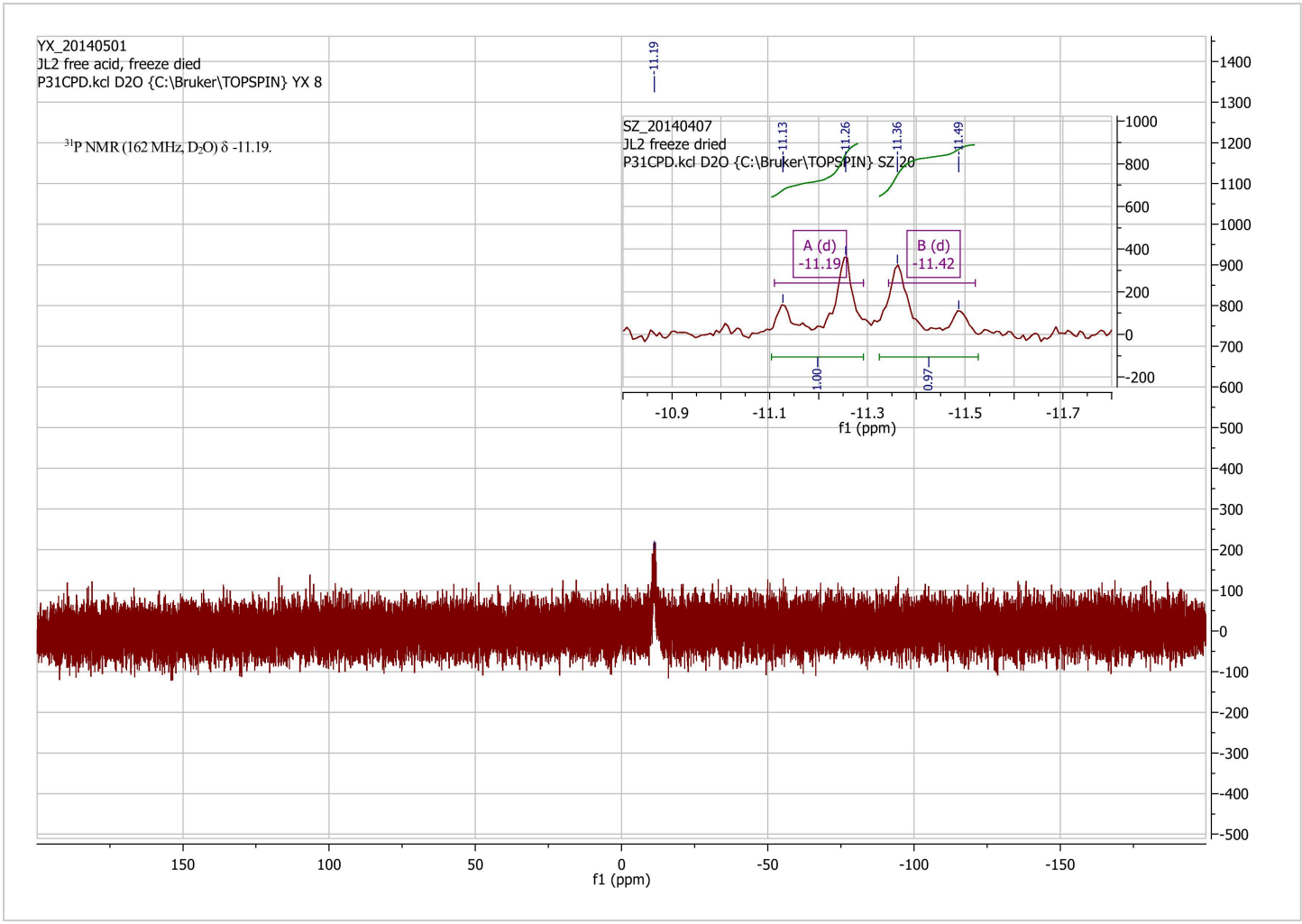

Figure 44: ^{31}P-NMR spectrum of ADPRumb

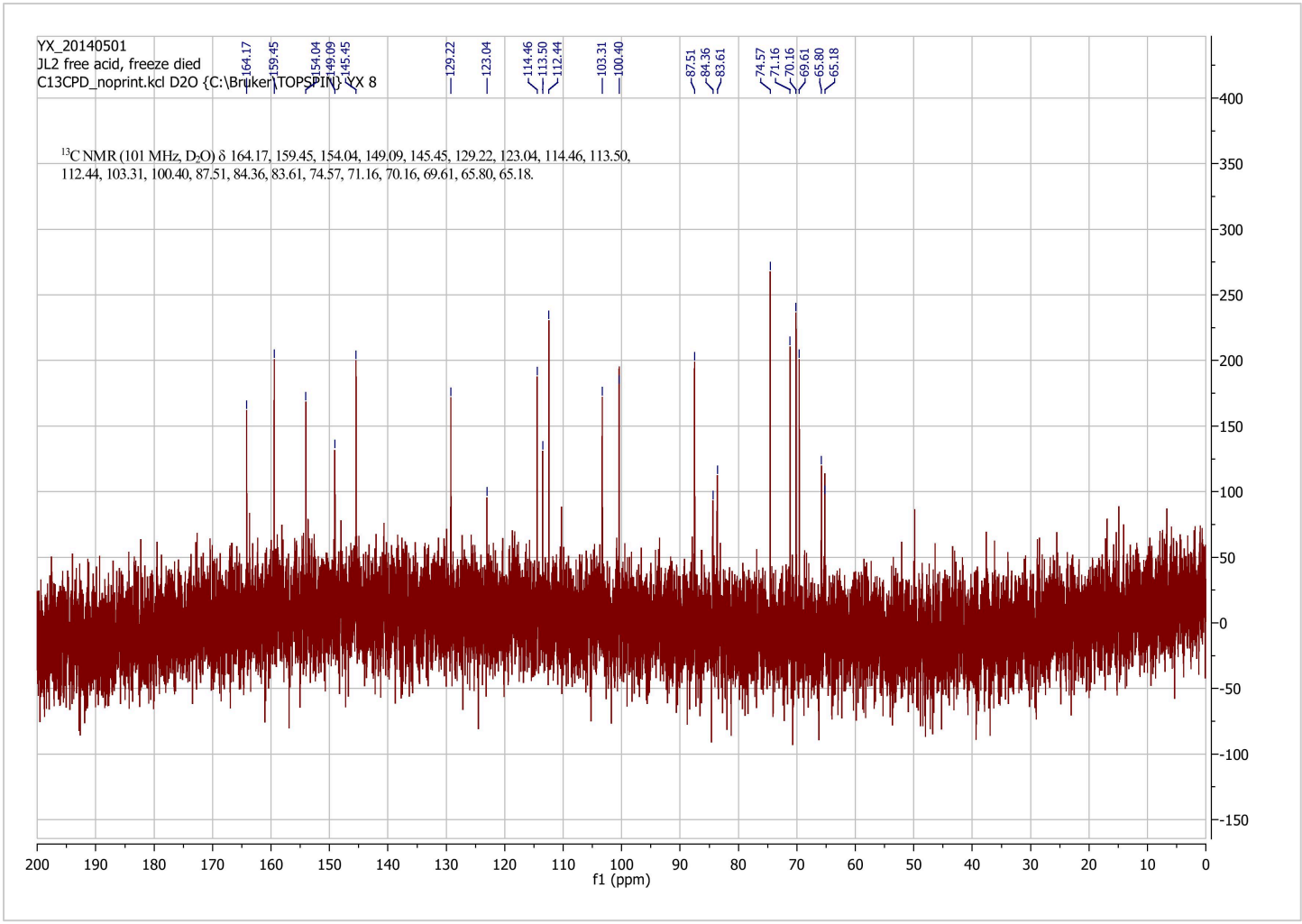

Figure 45: ^{13}C-NMR spectrum of ADPRumb

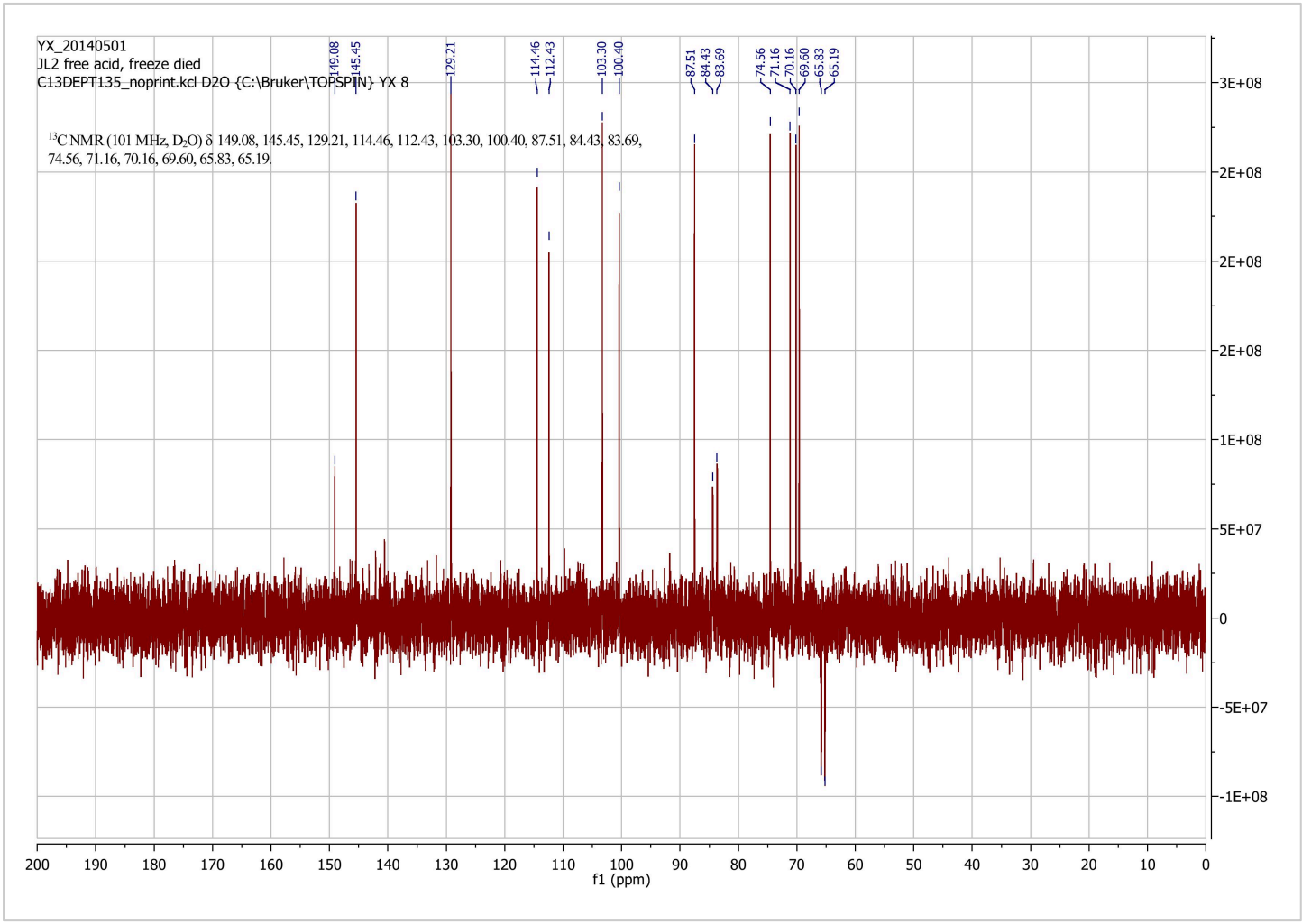

Figure 46: DEPT135 spectrum of ADPRumb

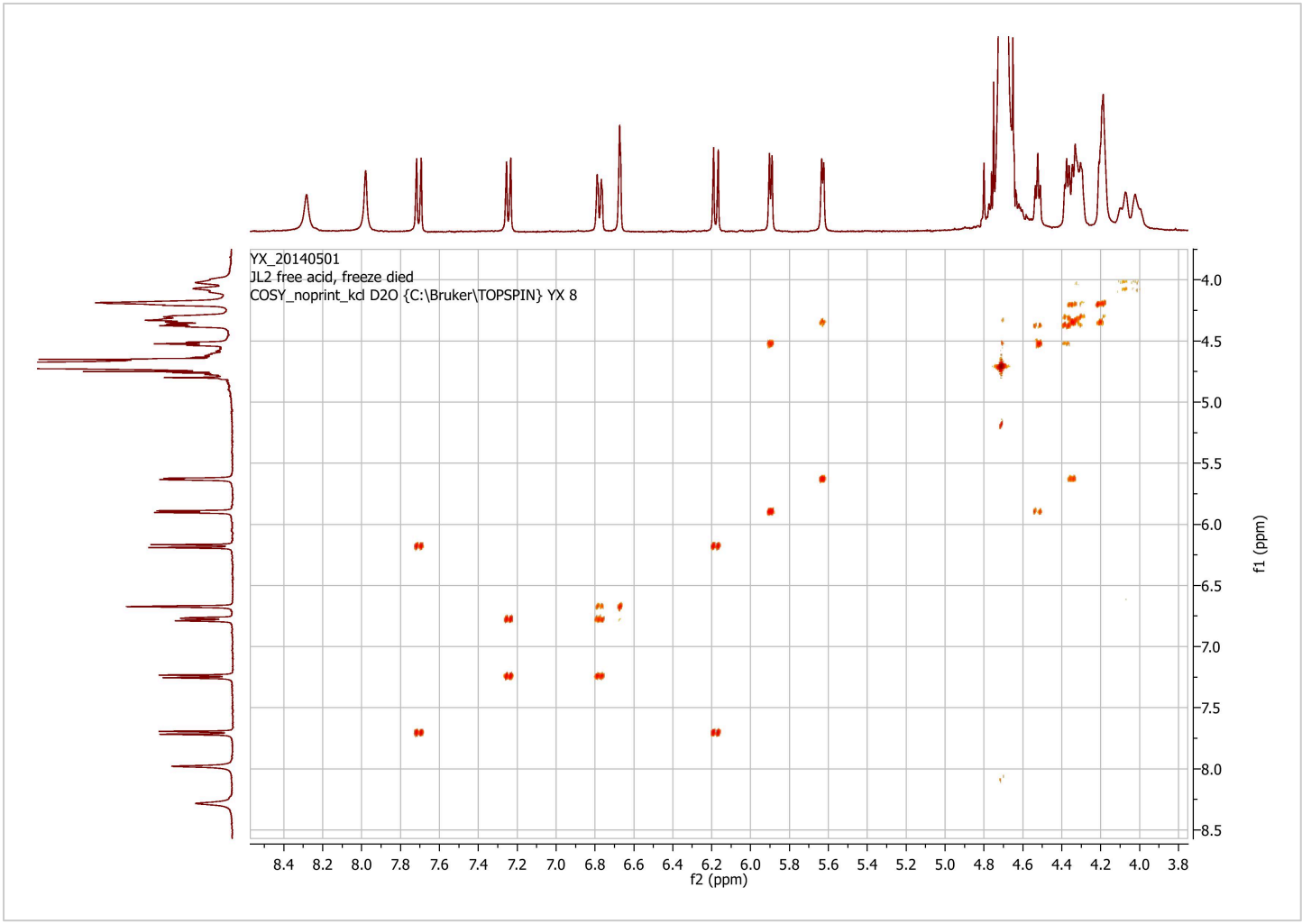

Figure 47: COSY spectrum of ADPRumb

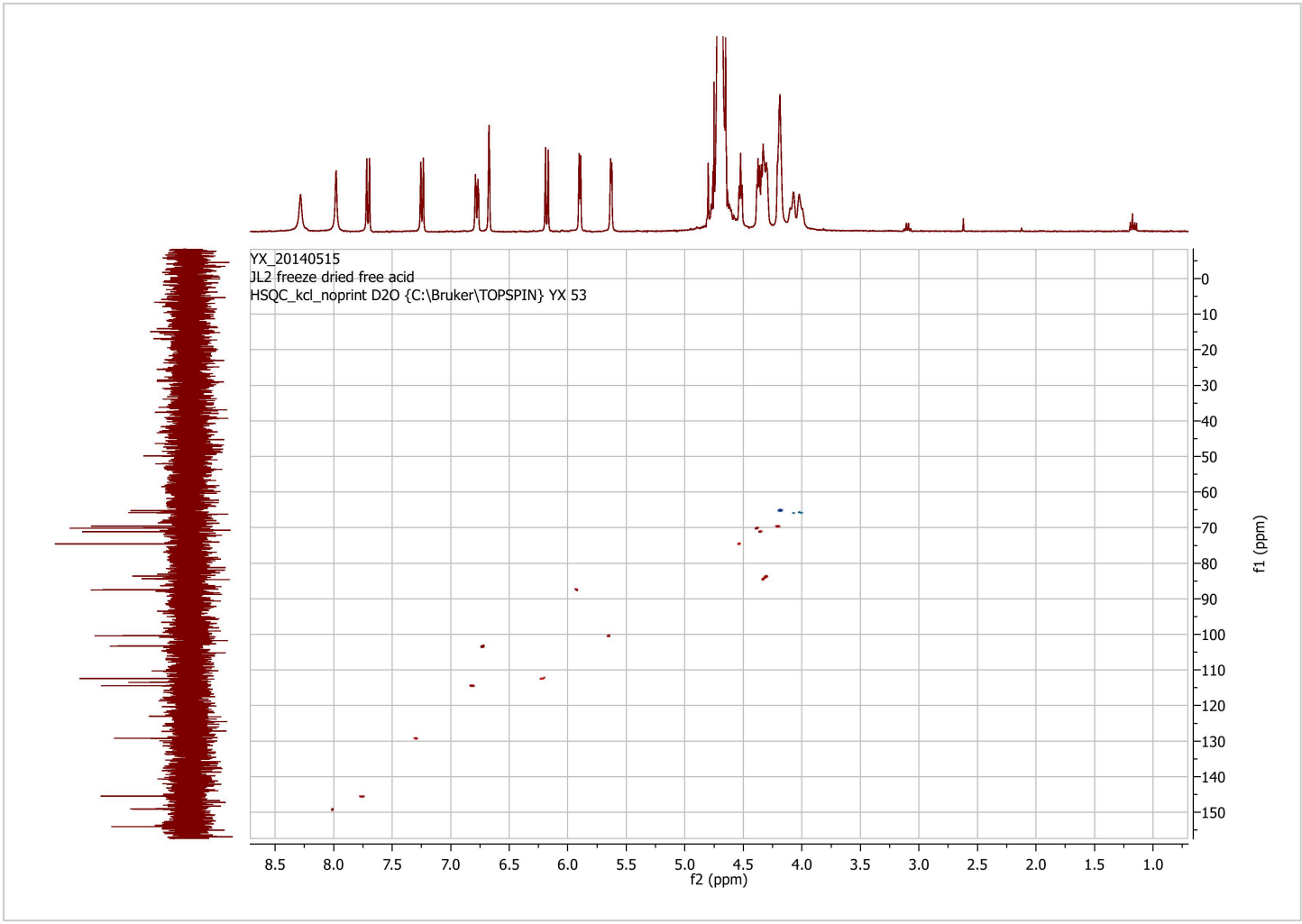

Figure 48: HSQC spectrum of ADPRumb

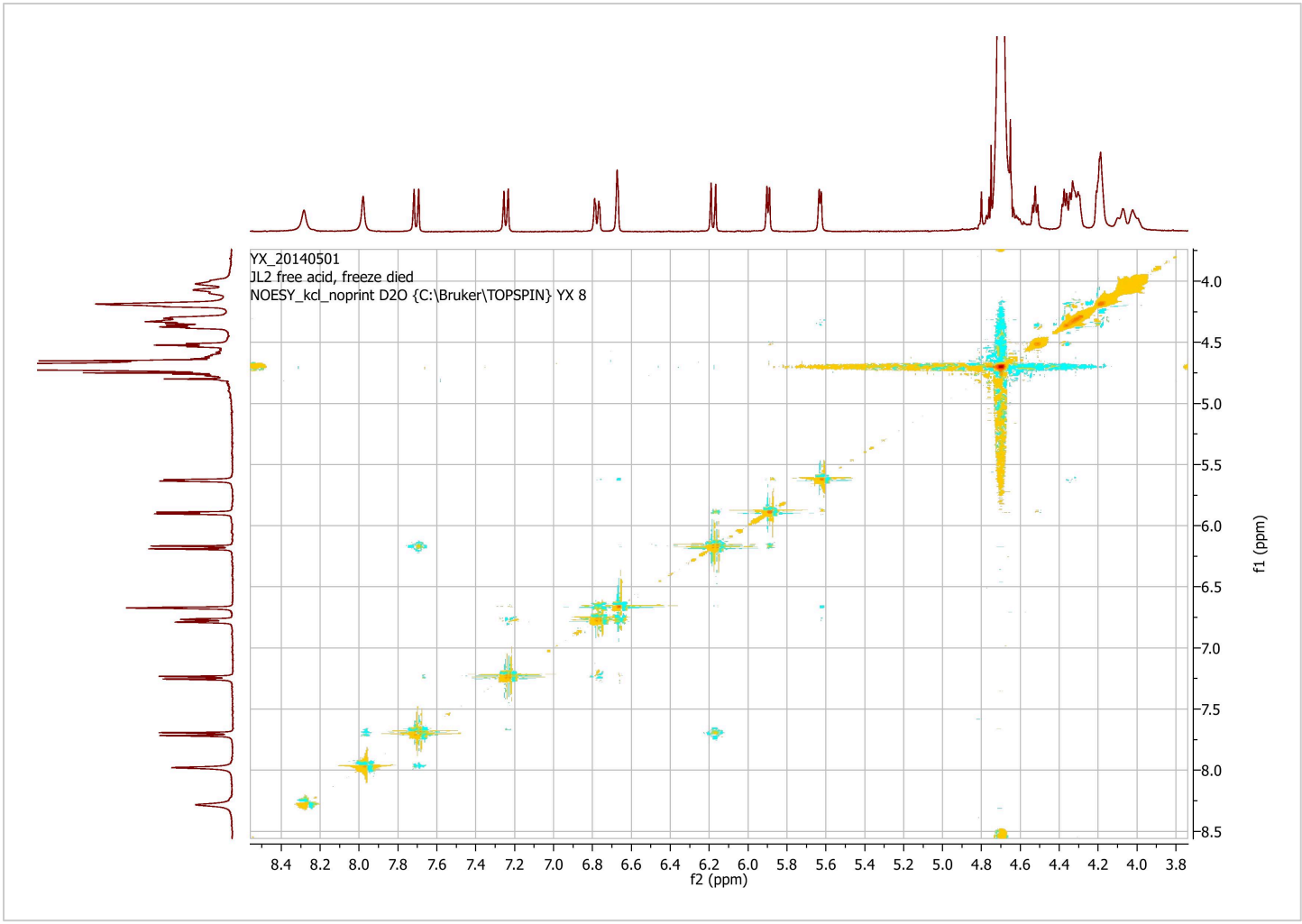

Figure 49: NOESY spectrum of ADPRumb

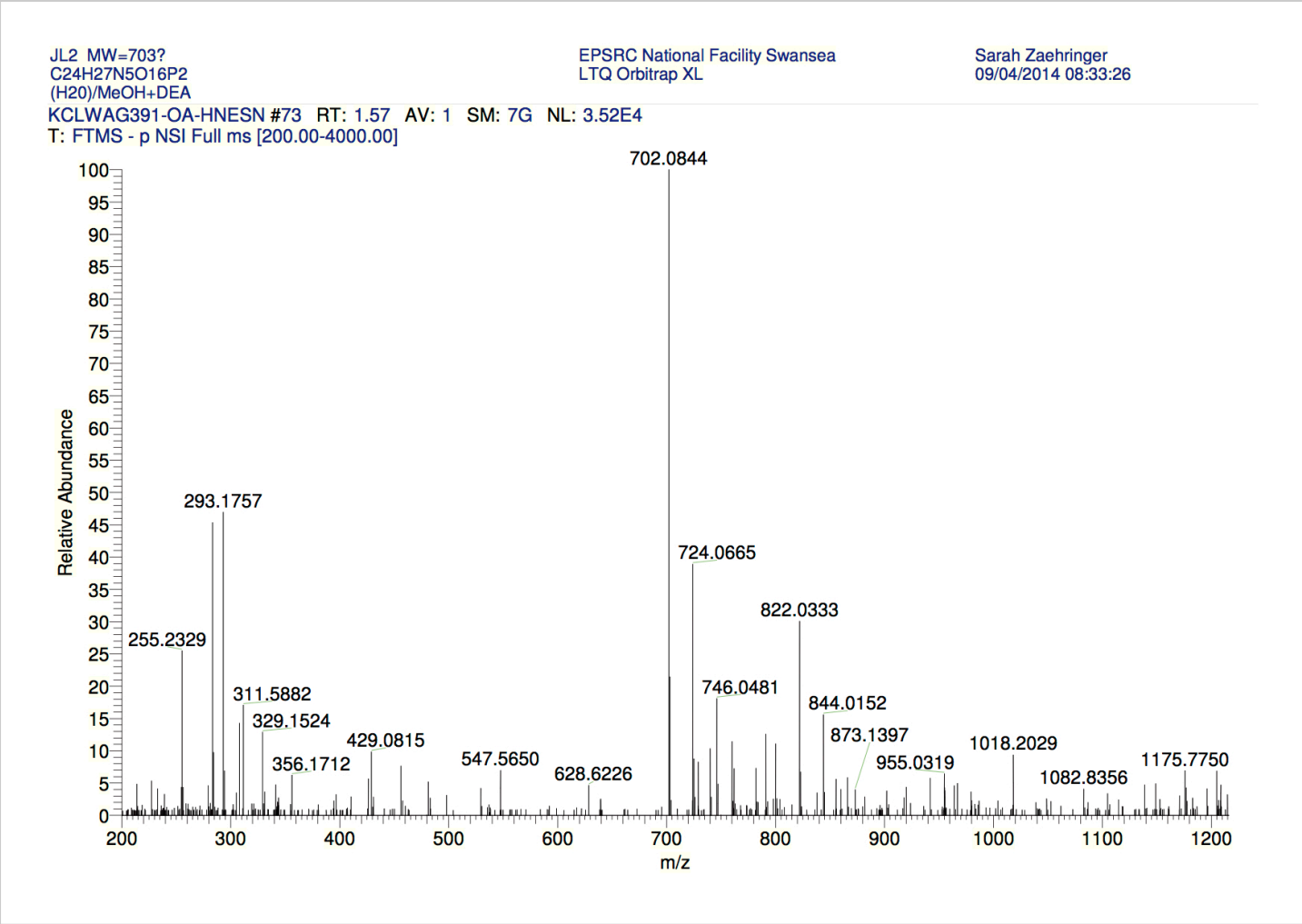

Figure 50: mass spectrum of ADPRumb

K) Appendix

K.1) List of Figures

K.2) List of Tables

K.3) List of Abbreviations

abs	absorbance
ADPR	adenosine diphosphate ribose
ADPR*p*NP	adenosine diphosphate ribose *para* nitrophenol
ADPRumb	adenosine diphosphate ribose umbelliferone
c	concentration
C-terminal	carboxy-terminal
cADPR	cyclic adenosine diphosphate ribose
CD	cluster of differentiation
CICR	calcium induced calcium release
CREB	cyclic adenosine monophosphate response element binding protein
d	doublet
DMSO	dimethyl sulfoxide

e.g.	exempli gratia, for example
eq	equivalent
ESI	electrospray ionisation
HEPES	4-(2-hydroxyethyl)-1-piperazineethanesulfonic acid
i.e.	id est, that is
J	coupling constant
LRX	liver X receptor
m	multiplet
NAADP	nicotinic acid ad
$NAD^{(+)}$	beta nicotinamide adenine dinucleotide (oxidised form)
NADH	beta nicotinamide adenine dinucleotide, reduced form
NADP	nicotinamide adenine dinucleotide phosphate
NMR	nuclear magnetic resonance
NOE	Nuclear Overhauser effect
NOESY	Nuclear Overhauser effect spectroscopy
P2Y1	purinergic receptor type P2Y1
p53	tumor suppressor p53
PGC	peroxisome proliferator activated receptor c coactivator
pK_a	acid dissociation constant
*p*NP	*para*-nitrophenol
poly(ADP)polymerase	poly adenosine diphosphate polymerase
ppm	parts per million
q	quartet
R_f	retention factor
RP	reversed phase
rpm	revolutions per minute
s	singlet
SIRT	sirtuin
SREBP	sterol regulatory element binding protein
std	standard deviation
t	triplet
TEAB	triethylammonium bicarbonate
TLC	thin layer chromatography

Tris	tris(hydroxymethyl)aminomethane
tRNA	transfer ribonucleic acid
TRPM2	transient potential receptor melastatin-2
U	unit
δ	chemical shift
λ_{max}	wavelength of maximum absorption/fluorescence
λ_{em}	wavelength of emission
λ_{ex}	wavelength of excitation

K.4) List of References

1. Zhao, X.; Allison, D.; Condon, B.; Zhang, F.; Gheyi, T.; Zhang, A.; Ashok, S.; Russell, M.; MacEwan, I.; Qian, Y.; Jamison, J. A.; Luz, J. G., The 2.5 Å Crystal Structure of the SIRT1 Catalytic Domain Bound to Nicotinamide Adenine Dinucleotide (NAD^+) and an Indole (EX527 Analogue) Reveals a Novel Mechanism of Histone Deacetylase Inhibition. *Journal of medicinal chemistry* **2013,** *56* (3), 963-969.
2. Verdin, E., The Many Faces of Sirtuins: Coupling of NAD metabolism, sirtuins and lifespan. *Nature Medicine* **2014,** *20* (1), 25-27.
3. Berger, F.; Ramírez-Hernández, M. a. H.; Ziegler, M., The new life of a centenarian: signalling functions of NAD(P). *Trends in Biochemical Sciences* **2004,** *29* (3), 111-118.
4. Honjo, T.; Nishizuka, Y.; Hayaishi, O.; Kato, I., Diphtheria Toxin-dependent Adenosine Diphosphate Ribosylation of Aminoacyl Transferase II and Inhibition of Protein Synthesis. *Journal of Biological Chemistry* **1968,** *243* (12), 3553-3555.
5. Lin, H., Nicotinamide adenine dinucleotide: beyond a redox coenzyme. *Organic & biomolecular chemistry* **2007,** *5* (16), 2541-2554.
6. Lee, H. C., Physiological Functions of Cyclic ADP-ribose and NAADPR as Calcium Messengers. *Annual review of pharmacology and toxicology* **2001,** *41* (1), 317-345.
7. Quan, S.; Imai, T.; Mikami, Y.; Yazawa, K.; Dabbs, E. R.; Morisaki, N.; Iwasaki, S.; Hashimoto, Y.; Furihata, K., ADP-Ribosylation as an Intermediate Step in Inactivation of Rifampin by a Mycobacterial Gene. *Antimicrobial Agents and Chemotherapy* **1999,** *43* (1), 181-184.
8. Prasad, G. S.; McRee, D. E.; Stura, E. A.; Levitt, D. G.; Lee, H. C.; Stout, C. D., Crystal structure of Aplysia ADP ribosyl cyclase, a homologue of the bifunctional ectozyme CD38. *Nature Structural & Molecular Biology* **1996,** *3* (11), 957-964.
9. Wei, W.; Graeff, R.; Yue, J., Roles and mechanisms of the CD38/cyclic adenosine diphosphate ribose/Ca^{2+} signaling pathway. *World journal of biological chemistry* **2014,** *5* (1), 58-67.
10. Hull, L. C.; Rabender, C.; Gabra, B. H.; Zhang, F.; Li, P. L.; Dewey, W. L., Role of CD38, a cyclic ADP-ribosylcyclase, in morphine antinociception and tolerance. *The Journal of pharmacology and experimental therapeutics* **2010,** *334* (3), 1042-50.
11. Yang, D.; Elner, S. G.; Chen, X.; Field, M. G.; Petty, H. R.; Elner, V. M., MCP-1-activated monocytes induce apoptosis in human retinal pigment epithelium. *Investigative ophthalmology & visual science* **2011,** *52* (8), 6026-34.
12. Yue, J.; Wei, W.; Lam, C. M. C.; Zhao, Y.-J.; Dong, M.; Zhang, L.-R.; Zhang, L.-H.; Lee, H.-C., CD38/cADPR/Ca^{2+} Pathway Promotes Cell Proliferation and Delays Nerve Growth

Factor-induced Differentiation in PC12 Cells. *Journal of Biological Chemistry* **2009,** *284* (43), 29335-29342.
13. Bruzzone, S.; Bodrato, N.; Usai, C.; Guida, L.; Moreschi, I.; Nano, R.; Antonioli, B.; Fruscione, F.; Magnone, M.; Scarfi, S.; De Flora, A.; Zocchi, E., Abscisic acid is an endogenous stimulator of insulin release from human pancreatic islets with cyclic ADP ribose as second messenger. *The Journal of biological chemistry* **2008,** *283* (47), 32188-97.
14. Galione, A.; Cui, Y.; Empson, R.; Iino, S.; Wilson, H.; Terrar, D., Cyclic ADP-ribose and the regulation of calcium-induced calcium release in eggs and cardiac myocytes. *Cell biochemistry and biophysics* **1998,** *28* (1), 19-30.
15. Sumoza-Toledo, A.; Penner, R., TRPM2: a multifunctional ion channel for calcium signalling. *The Journal of Physiology* **2011,** *589* (7), 1515-1525.
16. Gustafsson, A. J.; Muraro, L.; Dahlberg, C.; Migaud, M.; Chevallier, O.; Khanh, H. N.; Krishnan, K.; Li, N.; Islam, M. S., ADP ribose is an endogenous ligand for the purinergic P2Y1 receptor. *Molecular and Cellular Endocrinology* **2011,** *333* (1), 8-19.
17. Lee, H. C.; Aarhus, R., ADP-ribosyl cyclase: an enzyme that cyclizes NAD^+ into a calcium-mobilizing metabolite. *Cell regulation* **1991,** *2* (3), 203-9.
18. Zatman, L. J.; Kaplan, N. O.; Colowick, S. P.; Ciotti, M. M., The isolation and properties of the isonicotinic acid hydrazide analogue of diphosphopyridine nucleotide. *Journal of Biological Chemistry* **1954,** *209* (2), 467-484.
19. Muller-Steffner, H. M.; Augustin, A.; Schuber, F., Mechanism of Cyclization of Pyridine Nucleotides by Bovine Spleen NAD+ Glycohydrolase. *Journal of Biological Chemistry* **1996,** *271* (39), 23967-23972.
20. Wall, K. A.; Klis, M.; Kornet, J.; Coyle, D.; Amé, J. C.; Jacobson, M. K.; Slama, J. T., Inhibition of the intrinsic NAD^+ glycohydrolase activity of CD38 by carbocyclic NAD analogues. *Biochem. J.* **1998,** *335* (3), 631-636.
21. Sauve, A. A., Sirtuin chemical mechanisms. *Biochimica et biophysica acta* **2010,** *1804* (8), 1591-603.
22. Canto, C.; Sauve, A. A.; Bai, P., Crosstalk between poly(ADP-ribose) polymerase and sirtuin enzymes. *Mol. Asp. Med.* **2013,** *34* (6), 1168-1201.
23. Cantó, C.; Auwerx, J., Targeting Sirtuin 1 to Improve Metabolism: All You Need Is NAD^+? *Pharmacological Reviews* **2012,** *64* (1), 166-187.
24. Giblin, W.; Skinner, M. E.; Lombard, D. B., Sirtuins: guardians of mammalian healthspan. *Trends in Genetics* **2014,** *30* (7), 271-286.
25. Heltweg, B.; Trapp, J.; Jung, M., In vitro assays for the determination of histone deacetylase activity. *Methods* **2005,** *36* (4), 332-7.
26. Beher, D.; Wu, J.; Cumine, S.; Kim, K. W.; Lu, S. C.; Atangan, L.; Wang, M., Resveratrol is Not a Direct Activator of SIRT1 Enzyme Activity. *Chem. Biol. Drug Des.* **2009,** *74* (6), 619-624.
27. Smith, B. C.; Hallows, W. C.; Denu, J. M., A continuous microplate assay for sirtuins and nicotinamide-producing enzymes. *Analytical biochemistry* **2009,** *394* (1), 101-109.
28. Tarnus, C.; Muller, H. M.; Schuber, F., Chemical evidence in favor of a stabilized oxocarbonium-ion intermediate in the NAD^+ glycohydrolase-catalyzed reactions. *Bioorganic Chem.* **1988,** *16* (1), 38-51.
29. Berti, P. J.; Schramm, V. L., Transition State Structure of the Solvolytic Hydrolysis of NAD^+ *J. Am. Chem. Soc.* **1997,** *119* (50), 12069-12078.
30. Yamada, S.; Gu, Q.-M.; Sih, C. J., Cyclic ADP-Ribose via Stereoselective Cyclization of β-NAD *J. Am. Chem. Soc.* **1994,** *116* (23), 10787-10788.
31. Nottbohm, A. C.; Dothager, R. S.; Putt, K. S.; Hoyt, M. T.; Hergenrother, P. J., A Colorimetric Substrate for Poly(ADP-Ribose) Polymerase-1, VPARP, and Tankyrase-1. *Angewandte Chemie* **2007,** *119* (12), 2112-2115.

32. Fink, D. W.; Koehler, W. R., pH Effects on fluorescence of umbelliferone. *Analytical Chemistry* **1970,** *42* (9), 990-993.
33. Kaplan, N. O.; Colowick, S. P.; Barnes, C. C., Effect of alkali on diphosphopyridine nucleotide. *Journal of Biological Chemistry* **1951,** *191* (2), 461-472.
34. Cade-Menun, B. J., Characterizing phosphorus in environmental and agricultural samples by ^{31}P nuclear magnetic resonance spectroscopy. *Talanta* **2005,** *66* (2), 359-371.
35. Goodarzi, M.; Freitas, M. P.; Wu, C. H.; Duchowicz, P. R., pK_a modeling and prediction of a series of pH indicators through genetic algorithm-least square support vector regression. *Chemometrics and Intelligent Laboratory Systems* **2010,** *101* (2), 102-109.
36. Schwarzenbach, R. P.; Stierli, R.; Folsom, B. R.; Zeyer, J., Compound properties relevant for assessing the environmental partitioning of nitrophenols. *Environmental Science & Technology* **1988,** *22* (1), 83-92.
37. Sleath, P. R.; Handlon, A. L.; Oppenheimer, N. J., Pyridine coenzyme analogs. 3. Synthesis of three NAD$^+$ analogs containing a 2'-deoxy-2'-substituted nicotinamide arabinofuranosyl moiety. *J. Org. Chem.* **1991,** *56* (11), 3608-13.
38. Pergolizzi, G.; Butt, J. N.; Bowater, R. P.; Wagner, G. K., A novel fluorescent probe for NAD-consuming enzymes. *Chemical communications* **2011,** *47* (47), 12655-7.
39. Cakir-Kiefer, C.; Muller-Steffner, H.; Schuber, F., Unifying mechanism for Aplysia ADP-ribosyl cyclase and CD38/NAD$^+$ glycohydrolases. *Biochem. J.* **2000,** *349* (1), 203-210.
40. Ziegler, M.; Jorcke, D.; Zhang, J.; Schneider, R.; Klocker, H.; Auer, B.; Schweiger, M., Characterization of Detergent-Solubilized Beef Liver Mitochondrial NAD$^+$ Glycohydrolase and Its Truncated Hydrosoluble Form. *Biochemistry* **1996,** *35* (16), 5207-5212.
41. Baker, A., Fluorescence Excitation−Emission Matrix Characterization of Some Sewage-Impacted Rivers. *Environmental Science & Technology* **2001,** *35* (5), 948-953.
42. Gottlieb, H. E.; Kotlyar, V.; Nudelman, A., NMR Chemical Shifts of Common Laboratory Solvents as Trace Impurities. *The Journal of Organic Chemistry* **1997,** *62* (21), 7512-7515.

K.5) Curriculum vitae

Personal information

Name	Jakob Lausch
Date of birth	April 24, 1990
Place of birth	Vienna
Citizenship	Austria

Education

June 2008	Graduation from BG Hollabrunn
2009 – 2014	Diploma study in Pharmacy University of Vienna
March 2014 – July 2014	Diploma thesis Department of Chemistry and Institute of Pharmaceutical Sciences King's College London